Potent priming by inactivated whole influenza virus particle vaccines is linked to viral RNA uptake into antigen presenting cells.

Masashi Shingai[1,2,†], Naoki Nomura[1,†], Toshiki Sekiya[1,2,3,†], Marumi Ohno[1,†], Daisuke Fujikura[1,#], Chimuka Handabile[1], Ryosuke Omori[1], Yuki Ohara[4], Tomohiro Nishimura[4], Masafumi Endo[4], Kazuhiko Kimachi[4], Ryotarou Mitsumata[5], Tomio Ikeda[5], Hiroki Kitayama[6], Hironori Hatanaka[6], Tomoyoshi Sobue[7], Fumihito Muro[7], Saori Suzuki[8], Cong Thanh Nguyen[8], Hirohito Ishigaki[8], Misako Nakayama[8], Yuya Mori[8], Yasushi Itoh[8], Marios Koutsakos[2,3], Brendon Y Chua[2,3], Katherine Kedzierska[2,3], Lorena E Brown[2,3], David C Jackson[2,3], Kazumasa Ogasawara[8], Yoichiro Kino[9], and Hiroshi Kida[1,2,10 *]

[1] International Institute for Zoonosis Control, Hokkaido University, Sapporo, Japan.
[2] International Collaboration Unit, International Institute for Zoonosis Control, Hokkaido University, Sapporo, Japan.
[3] The Department of Microbiology and Immunology, The University of Melbourne at the Peter Doherty Institute for Infection and Immunity, Melbourne, Australia.
[4] KM Biologics Co. Ltd., Kumamoto, Japan
[5] Denka Co., Ltd., Niigata, Japan.
[6] BIKEN Co., Ltd., Kannonji, Japan.
[7] Daiichi Sankyo, Co, Ltd, Tokyo, Japan.
[8] Division of Pathgenesis and Disease Regulation, Department of Pathology, Shiga University of Medical Science, Otsu, Japan.
[9] Kino Consulting, Kumamoto, Japan
[10] Collaborating Research Center for the Control of Infectious Diseases, Nagasaki University, Nagasaki, Japan.

† equally contributed to the present study.
# present address is School of Veterinary Medicine, Kitasato University, Towada, Japan
* Corresponding author: Hiroshi Kida
International Institute for Zoonosis Control, Hokkaido University, Kita-20 Nishi-10, Kita-ku, Sapporo 001-0020, Hokkaido, Japan
Tel: +81-11-706-9500; FAX: +81-11-706-9500
E-mail: kida@vetmed.hokudai.ac.jp

Running title
Superior priming potency of inactivated whole influenza virus particle vaccine to current ether-split vaccine

Key words
Inactivated whole influenza virus particle vaccine; seasonal and pandemic influenza.

1. Introduction

Influenza is a highly contagious respiratory illness that is responsible for significant morbidity and mortality. Over 1 billion cases are reported each year, 3 to 5 million of which are severe and result in 290,000 to 650,000 deaths annually worldwide [1-3]. Adults 65 years and older are at particular risk of severe disease, hospitalization, and mortality due to seasonal influenza [4]. Young children are also at risk due to higher attack rates [5, 6]. Children are key virus spreaders in a community because they are more susceptible to influenza virus infection than adults and frequently make contact with friends and family members, resulting in shedding larger amounts of virus in the community over a long period of time [7, 8]. In fact, the best predictor for influenza occurring in a household is the presence of children [9, 10]. Thus, children should be prioritized for prevention of influenza through vaccination.

Annual vaccination is the most effective way to prevent influenza and to reduce an individual's risk of severe influenza-related disease. The first inactivated seasonal influenza vaccine was developed as a whole virus particle vaccine (WPV) in the 1940s and was used for 30 years [11]. However, the administration of the WPV vaccine to children occasionally caused side effects such as fever, pain, and fatigue [12, 13], which led many people to mistakenly assume that the vaccine might cause flu-like symptoms. One of the reasons for this reactogenicity was thought to be due to impurities, such as egg-derived contaminants, in the vaccine [13]. Therefore, the manufacturing process for the newly developed seasonal influenza vaccines had an additional purification step to remove the impurities using zonal centrifugation. Moreover, most current influenza vaccines are disrupted using ether and/or detergents to decrease febrile reactions, hence the name "split" vaccine (SV). Several clinical trials demonstrated that SV was indeed less pyrogenic than WPV but was also less immunogenic, especially in young children [14-16]. Despite some disagreements, SV was approved in the United States as a standard influenza vaccine and replaced WPV in 1968 [11], and in Japan in 1972. A report of a clinical trial by Gross *et al.* [15, 16] highlighted three interesting findings: 1) in young children WPV causes fever more frequently than does SV, 2) young children previously vaccinated with influenza virus vaccine are unlikely to experience fever subsequent to immunization with a related antigen and 3) SV induces less vaccine strain-specific antibodies than does WPV in immunologically unprimed young children. The fact that WPV but not SV induces immunity in "naïve" children with a febrile response implies that the fever caused by WPV accompanies immune priming responses.

To re-evaluate WPV, we established the All Japan Influenza Vaccine Study Group and requested that member vaccine manufacturers in Japan prepare WPV and SV from the same purified virus batches from which egg-derived contaminants had been removed. Our previous study utilizing such matched sets of WPV and SV preparations demonstrated the superiority of WPV over SV in terms of the induction of neutralizing antibodies and $CD8^+$ T cell responses in naïve mice as well as protection against severe disease following homologous virus challenge [17]. These results not only encouraged us to advance this project to preclinical study, but also raised a new question as to why WPV, rather than SV, elicits an effective priming response. To address this question, we compared priming and boosting effects of WPV and SV in cynomolgus macaques. The present study provides data

supporting the strong priming effect of WPV compared to SV and provides evidence for the mechanistic basis that underpins this phenomenon.

2. Material and methods

2.1 Cells and viruses

Madin-Darby canine kidney (MDCK) cells were grown in RP10 (RPMI 1640; Thermo Fisher Scientific, MA, USA) supplemented with 10% inactivated fetal calf serum (FCS) (GE Healthcare UK Ltd, Little Chalfont, Buckinghamshire, UK), 1 mM of sodium pyruvate (Thermo Fisher Scientific), 50 μM of 2-mercaptoethanol (Merck, Darmstadt, Germany), 100 U/ml of penicillin (Thermo Fisher Scientific), 100 μg/ml of streptomycin (Thermo Fisher Scientific), and 20 μg/ml of gentamicin (Thermo Fisher Scientific). These were used for neutralization assays and plaque assays. Influenza viruses A/Singapore/GP1908/2015 (IVR-180) (H1N1), A/California/7/2009 (X-179A) (H1N1) pdm09, A/Hong Kong/4801/2014 (X-263) (H3N2), B/Phuket /3073/2013 (Yamagata linage), and B/Texas/2/2013 (Victoria lineage) were kindly provided by the National Institute of Infectious Diseases in Japan. Viruses were propagated in 10-day-old embryonated chicken eggs. The collected allantoic fluids were stored at -80°C until use.

2.2 Vaccines

WPV and SV used in this study were prepared by vaccine manufacturers in Japan [17]. Quadrivalent vaccine contained antigens from influenza virus vaccine strains used in 2017-2018, namely A/Singapore/GP1908/2015 (IVR-180) (H1N1), A/Hong Kong/4801/2014 (X-263) (H3N2), B/Phuket /3073/2013 (Yamagata linage), and B/Texas/2/2013 (Victoria lineage). The monovalent vaccine contained antigens from A/California/7/2009 (X-179A) (H1N1) pdm09. Vaccine virus strains were propagated in embryonated chicken eggs and highly purified from the allantoic fluids through sucrose density gradient centrifugation [18]. In the present study, the highly purified virions were inactivated with formalin and/or β-propiolactone to prepare WPVs according to the standard methods used by vaccine manufacturers [17]. SVs were prepared by disrupting the purified virions with ether, according to the license for current seasonal influenza vaccine production. HA protein concentrations of WPV and SV were measured using a single-radial-immunodiffusion method. In addition, WPVs in this study showed almost equivalent chicken cell agglutination (CCA) values to the classical WPVs. Influenza vaccines were subcutaneously injected to animals as in our previous report.

2.3 Animals

Female C57BL/6 mice were purchased from Hokudo Co., Ltd. (Sapporo, Japan) and kept in a BSL-2 laboratory at the Research Center for Zoonosis Control, Hokkaido University. Either quadrivalent WPV (3, 1.2, 0.6, and 0.3 μg HA protein per each vaccine strain) or SV (3 μg HA protein per each vaccine strain) was injected subcutaneously into 7-week-old female C57BL/6 mice under inhalation anesthesia with isoflurane. Serum samples were collected on day 24 after injection to estimate neutralizing antibody titers. On day 28 after injection, mice were challenged with an intranasal infection of 3,000 plaque forming units (PFUs) of A/Singapore/GP1908/2015 (IVR-180) (H1N1) in 40 μl of phosphate buffered

saline (PBS) as a 100% lethal dose under inhalation anesthesia with isoflurane. Body weight was monitored daily after infection. Lungs were harvested 5 days post infection and homogenized in $RPMI_{anti}$ (RPMI 1640 medium supplemented with 100 U/ml penicillin, 100 µg/ml streptomycin and 20 µg/ml gentamicin) and centrifuged at 2,000rpm to obtain supernatant, and stored at -80°C until use.

A total of 61 healthy female and male cynomolgus macaques (*Macaca fascicularis*) imported from Cambodia, aged around 3 years and weighing 2-5 kg, were used for the experiments. Monkeys were singly housed in steel cages measuring 68-cm-deep by 62-cm-wide by 77-cm-high in a ventilated animal room with controlled temperature (23 to 29°C), relative humidity (30 to 70%), and 12 hr of light (7:00 to 19:00) at Shin Nippon Biomedical Laboratories, Ltd (Kagoshima, Japan). Macaques were vaccinated subcutaneously with quadrivalent WPV or SV. Blood samples were collected in heparin tubes at indicated timepoints, and plasma for the measurement of neutralizing antibody titers was separated and stored at -80°C until use. Throughout the experiments, all efforts were made to minimize the suffering of animals.

Current SV for human use contains 15 µg HA for each strain. In this study macaques and mice received WPV containing HA of 1/8 to equivalent amount and 1/50 to 1/5 amount, respectively, compared with a dose applied in humans.

2.4 Ethics statement

All mouse experiments were performed with approval (Approval No. 17-0003) from the Animal Care and Use Committee of Hokkaido University following Fundamental Guidelines for Proper Conduct of Animal Experiment and Related Activities in Academic Research Institutions under the jurisdiction of the Ministry of Education, Culture, Sports, Science and Technology in Japan.

All monkey experiments had been approved by the Institutional Animal Care and Use Committee (Approval No. IACUC718-007, 008, and 009) and carried out in strict accordance with animal welfare regulations of Shin Nippon Biomedical Laboratories, Ltd., Drug Safety Research Laboratories, which is accredited by the Association for Assessment and Accreditation of Laboratory Animal Care (AAALAC) International.

2.5 Measurement of virus titers in the lungs of mice by plaque assay

Virus titers in the lung supernatants of infected mice were determined by a plaque assay. MDCK cells were seeded into 6-well tissue culture plates at a density of 1.2×10^6 cells per well and incubated overnight at 37°C in 5% CO_2. Cell monolayers were washed with $RPMI_{anti}$ and 125 µl of lung supernatant, diluted from 10^{-1} to 10^{-3} in $RPMI_{anti}$, was added to each well. After incubation of the plate for 45 min at 37°C in 5% CO_2, 3 ml of warmed (45°C) overlay medium consisting of Leibovitz L-15 with glutamine at pH 6.8 (Thermo Fisher Scientific) supplemented with 0.028% (w/v) $NaHCO_3$ (Merck), 100 IU/ml penicillin, 100 mg/ml streptomycin, 0.1% (w/v) TPCK-treated trypsin (Merck), and 0.9% (w/v) agarose (Merck) was then added to each well. The plates were incubated for 3 days at 37°C in 5% CO_2. Plaques formed on monolayers were counted and the number of plaque-forming units (PFU) in the original lung sample was calculated.

2.6 Receptor-destroying enzyme (RDE) treatment of the sera of mice and monkeys and hemagglutination inhibition (HI) assay

To reduce inhibition of hemagglutination by non-specific inhibitors, the sera were treated with RDE II (Denka, Tokyo, Japan) at a ratio of 1:3 (serum: RDE) and then incubated overnight at 37ºC. After inactivation of RDE by incubation at 56ºC for 1 hr, phosphate buffered saline (PBS) was added at 4 times the volume of the serum (the final ratio of serum:RDE:PBS is 1:3:6) to give a starting dilution of 1:10. Serial two-fold dilutions of the RDE-treated sera in PBS were carried out in Round bottom 96-well microplates. The diluted sera were mixed with 8 hemagglutinin units of virus antigen [A/Singapore/GP1908/2015 (IVR-180) (H1N1), A/California/7/2009 (X-179A) (H1N1) pdm09, A/Hong Kong/4801/2014 (X-263) (H3N2), B/Phuket /3073/2013 (Yamagata linage), or B/Texas/2/2013 (Victoria lineage)] and incubated at room temperature (RT) for 30 min. An equal volume of 0.5% suspension of chicken red blood cells were added to the antigen-serum dilution mixtures and incubated at RT for 30 min. HI titers were expressed as reciprocals of the highest serum dilutions that showed complete inhibition of hemagglutination.

2.7 Neutralization assay of the sera of mice

Neutralizing antibody titers of RDE-treated mouse sera were measured in a plaque reduction assay. Monolayers of MDCK cells were prepared by seeding 1.2×10^6 cells in 3 ml of RP10 medium in each well of a 6-well tissue culture plate and incubated overnight at 37°C in 5% CO_2. Serial ten-fold dilutions of the RDE-treated sera in PBS were carried out in 96-well microplates. An equal volume of influenza virus was then added to each serum dilution to give a final concentration of 100 PFU/100 µl and the mixtures incubated for 1 hr at RT. Cell monolayers were washed with $RPMI_{anti}$ then 100 µl of virus-serum mixtures added. Any non-neutralized virus was allowed to adsorb for 45 min during which time the plates were shaken gently at 15 min intervals. Warmed (45°C) overlay medium (3 ml/well) was then added to each well. The plates were incubated at 37°C in 5% CO_2 for 3 days and plaques on the monolayers were counted without staining. The virus neutralizing antibody titers were expressed as the reciprocal of the highest serum dilutions that reduced the number of plaques to 50% of that obtained in control wells that had no serum.

2.8 Micro-neutralization Enzyme-Linked Immunosorbent Assay (ELISA) of macaque sera

RDE-treated macaque sera were serially 2-fold diluted with PBS in 96-well microplates. The diluted sera were mixed with an equal volume of virus (100 $TCID_{50}$) and the virus-serum mixtures were incubated at 37°C for 1 hr. MDCK cell suspensions containing 1×10^6 cells in 100 µl were added to 50 µl of virus-serum mixture and incubated in 96-well plates in the presence of 1 µg/ml TPCK-trypsin at 37°C for 24 hr. Cell monolayers were washed with PBS and fixed in cold 80% acetone for 15 min. The presence of nucleoprotein (NP) of influenza virus was detected by ELISA with a specific monoclonal antibody (HB65/H16-L10-4RS: BioXCell, Lebanon, NH, USA).

The ELISA was performed at RT. The fixed monolayers were washed three times with PBS containing 0.05% Tween 20 (wash buffer). After incubation for 1hr with a blocking buffer containing 1% of bovine serum albumin (BSA) in PBS, the anti-NP antibody diluted to

1/6,000 in blocking buffer was added to each well. The plates were incubated at RT for 1 hr. The plates were washed three times with wash buffer, and 100 µl of horseradish peroxidase-labeled goat anti-mouse immunoglobulin G (IgG) (Thermo Fisher Scientific) diluted to 1/6,000 in blocking buffer was added to each well. The plates were incubated for 1 hr at RT and then washed three times with wash buffer. One hundred microliters of freshly prepared substrate using SIGMAFAST™ OPD (Thermo Fisher Scientific) was added to each well, and the plates were incubated at RT for 15 min. The reaction was stopped by the addition of 50 µl of 2N sulfuric acid. The absorbance at 490 nm (A490) was measured with a microplate reader. The intermediate OD value was determined from quadruplicate wells of virus-infected and uninfected control wells, and the neutralization titer was determined as the maximum dilution below the intermediate OD value.

2.9 Cytokine detection in CD14 positive cells and CD14 depleted cells from cynomolgus macaques

Spleens were collected from unimmunized macaques at autopsy, homogenized, and stored at -80^{o} C until use. CD14^{+} splenocytes were isolated using CD14 microbeads for magnetic cell sorting (MACS, Miltenyi Biotec GmbH, Bergisch Gladbach, Germany). The remaining splenocytes were used as CD14-depleted splenocytes. The cells (5×10^5 of CD14-depleted splenocytes or 1×10^5 of CD14^{+} splenocytes) were cultured in the presence of the vaccine preparations (3 µg/ml of HA proteins) or lipopolysaccharide (LPS, 1 mg/ml) for 6 hr. Levels of cytokines in supernatants were measured using a MAGPIX Milliplex MAP kit for nonhuman primate (Merck) and a Luminex 200 system (Millipore Corp., Billerica, MA).

2.10 Cytokine detection in dendritic cells (DCs) from mice

Mouse DCs were isolated from single cell suspensions of spleen, using CD11c micro beads (Miltenyi Biotec GmbH) according to the manufacturer's instructions. One million DCs were suspended in 100 µl of RP10 in 96-well round-bottom tissue culture plates and immediately stimulated with WPV or SV preparations containing 0.5 µg HA. PBS was used as a non-stimulation control. Total RNA was extracted from the cells at 6 hr post-stimulation for mRNA analysis as described below. Culture supernatants were collected at 24 hr post-stimulation for cytokine analysis. Concentrations of cytokines and chemokines (IFN-γ, IL-6, TNF-α, IP-10 and MCP-1) were determined using a MAGPIX Milliplex kit (Merck) according to instructions of the manufacturer. Briefly, 50 µl of culture supernatants, positive control samples, and standards for calibration curve were added to a 96-well plate. Magnetic beads coated with the antibodies against the target cytokines and chemokines were added into each well and the plate was incubated on a plate shaker overnight at 4°C. After washing with wash buffer provided in the kit, the samples were reacted with biotinylated detection antibodies for 1 hr and then streptavidin-phycoerythrin for 30 min. After washing with the wash buffer and addition of loading buffer from the kit, the samples were analyzed by a MAGPIX system (Luminex, Austin, TX).

2.11 RNA extraction and Quantitative-PCR (qPCR)

Total RNA was extracted from cells or vaccine solutions using Trizol LS reagent (Thermo Scientific) according to the manufacturer's instructions. The concentration of extracted RNA in each vaccine was estimated using a Nanodrop spectrophotometer (Thermo Scientific, Wilmington, DE, USA). Complementary DNA was synthesized from the extracted total RNA using random hexamer and ReverTra Ace® qPCR RT Master Mix (Toyobo, Osaka, Japan) according to the manufacture's instructions. To determine the RNA copy number, real time qPCR was performed using a SYBR Premix Ex Taq II kit (Tli RNaseH Plus, Takara Bio, Otsu, Japan) in a CFX96 system (BioRad, Hercules, CA). The primer sequences for target genes were as follows: For mouse IP10 (CXCL10) gene, forward primer is 5'- GGATCCCTCTCGCAA-3' and reverse primer is 5'- ATCGTGGCAATGATC-3'. For mouse IFN-α gene, forward primer is 5'-TCTGATGCAGCAGGTGGG-3' and reverse primer is 5'-AGGGCTCTCCAGACTTCTGCTCTG-3'. For mouse IFN-β gene, forward primer is 5'-CAGCTCCAAGAAAGGACGAAC-3' and reverse primer is 5'-GGCAGTGTAACTCTTCTGCAT-3'. For influenza A virus NP segment, forward primer is 5'-GATTGGTGGAATTGGACGAT-3' and reverse primer is 5'-AGAGCACCATTCTCTCTATT-3'. To determine the RNA copy number incorporated into DCs, $1x10^5$ CD11c-positive DCs from mouse spleens were inoculated with WPV or SV containing 5 μg of HA. After an hr incubation, the DCs were washed twice with ice-cold PBS and total RNA was extracted for reverse transcription and qPCR as described earlier.

2.12 Fluorescent staining and *in situ* hybridization

Mouse splenic $CD11c^+$ DCs were cultured overnight on Labtek chamber slides II (Nalge *Nunc* Int., Wiesbaden, Germany) and the cells were exposed to WPV or SV, the amounts of which had been adjusted to provide equivalent copy numbers of the viral NP gene segment (5×10^5 copies). Live virus, at multiplicity of infection (MOI) of 10, was used as a positive control. After 3 hr incubation, viral NP segments on the slides were stained using a ViewRNA ISH Cell Assay Kit (Affymetrix, Santa Clara, CA, USA) with a fluorescein-conjugated NP segment specific probe (Affymetrix) and DAPI according to the manufacturer's instructions. The fluorescent signals on the slides were detected using a Zeiss 780 LSM confocal microscope (Carl Zeiss, Jena, Germany), and colocalization was analyzed using ZEN 2011 software (Carl Zeiss).

2.13 Evaluation of CD86 expression on DCs by flow cytometry

Lymph nodes were collected from mice 6-48 hr after vaccination with WPV or SV and single cell suspensions prepared in RP10. Lymph node cells were stained with PE-conjugated anti-CD86 (clone; GL-1), fluorescein-conjugated anti-CD11c (clone; HL3), PerCP5.5-conjugated anti-CD19 (clone; 6D5), Alexa Fluor 700-conjugated anti-B220 (clone; RA3-6B2) and BV421-conjugated anti-CD11b (clone; M1/70) antibodies, following Fc-block with anti-CD16/32 (clone; 93) antibody. After washing twice with ice-cold PBS containing 0.5% BSA and 0.1% NaN_3, the cells were further stained with 7AAD (BioLegend, San Diego, CA). Fluorescent intensities of the cells were detected on an LSR Fortessa system (BD Biosciences, San Jose, CA). Conventional dendritic cells (cDCs) were determined as 7AAD negative, CD19 negative, CD11b positive, CD11c positive and B220 negative. Plasmacytoid dendritic cells (pDCs) were determined as 7AAD negative, CD19 negative,

CD11b negative, CD11c positive and B220 positive. The CD86 expression on cDCs and pDCs were analyzed using FlowJo software (Treestar, Ashland, OR). All antibodies were purchased from Biolegend.

2.14 Statistical analysis

Prism 7 (GraphPad Software, San Diego, CA, USA) was used to perform statistical analyses. *P* values were obtained using one-way ANOVA or two-way ANOVA with multiple comparisons or unpaired *t*-test. A *p* value less than 0.05 was considered statistically significant.

3. Results

3.1 The priming potency of quadrivalent WPV is greater than that of the corresponding SV.

Our previous study demonstrated that a single inoculation of monovalent WPV induced protective immunity in naïve mice, whereas monovalent SV did not, indicating that WPV but not SV has the capacity to prime an immune response in naïve animals [17]. Since quadrivalent not monovalent vaccines are routinely used in humans, we conducted similar experiments in a mouse model utilizing quadrivalent WPV and SV prepared by the same manufacturer. Mice were vaccinated with different amounts of WPV (0.3, 0.6, 1.2, or 3 μg HA/strain), SV (3 μg HA/strain) or PBS, and then infected with 3,000 PFU of homologous influenza virus A/Singapore/2015 (H1N1) on day 28 after vaccination. To evaluate the ability of vaccine-induced immunity to reduce virus replication, virus titers in the lungs on day 5 after virus challenge were examined. Pulmonary virus titers of mice inoculated with PBS were approximately 10^6 PFU (Figure 1a). When comparing SV and WPV containing the same amount of HA (3 μg) to the PBS group, the virus titers in the lungs were reduced approximately ten-fold on average in SV vaccinated mice, whereas the virus was barely detectable ($< 10^2$ PFU) in WPV vaccinated mice. In addition, suppression of the virus titers in the lungs observed in WPV-vaccinated groups showed a dose-dependency. Body weight changes, one of the indicators for disease severity, were also monitored daily until 5 days post-infection (dpi). Body weight of mice inoculated with SV or PBS decreased to around 80% of starting weight at 5 dpi (Figure 1b). In contrast, mice vaccinated with WPV containing 3 μg HA showed little body weight loss after virus challenge. Body weight loss of mice vaccinated even with diluted WPV only reached low levels, significantly less than the SV group, which received 10-times the vaccine dose. The severity of weight loss appeared to correlate with virus titers in the lungs of mice. To evaluate potency of WPV and SV to induce protective antibodies, neutralizing antibody titers in the sera of mice sampled on day 24 were measured against the homologous virus, A/Singapore/2015 (H1N1). In PBS-treated mice, serum neutralizing antibody titers were under the detection limit (Figure 1c). There was no significant difference in the titer between PBS- and SV-treated groups. In contrast, neutralizing antibody levels were significantly greater in mice immunized with the same HA dose of WPV than of SV. Furthermore, data of diluted WPVs demonstrated that the neutralizing antibody response induced by WPV was dose-dependent and negatively correlated with virus titers in the lungs. These results confirmed strong priming potency of the quadrivalent WPV as observed for a monovalent WPV previously [17].

We further investigated the potency of WPV and SV to prime and boost protective immune responses in cynomolgus macaques, which are biologically more closely related to humans than are mice (Figure 2). Naïve cynomolgus macaques were vaccinated on day 0 and 28 with either WPV or SV as shown in Figure 2. Plasma samples were collected on day 0, 28, and 49 to evaluate antibody titers against the vaccine strains. On day 28 after the first vaccination, HI antibodies against influenza A virus vaccine strains, A/Singapore/2015 (H1N1) and A/Hong Kong/2014 (H3N2), were induced only in macaques vaccinated with WPV (left and middle data in Figure 2a and b). HI titers against influenza B virus vaccine strains, B/Phuket/2013 (Yamagata linage) and B/Texas/2013 (Victoria linage), showed a similar tendency (Figure 2c and 2d). In contrast, one inoculation of SV did not induce HI antibodies against any of the virus strains. These data from the cynomolgus macaque model mirrors the ineffective and effective priming by SV and WPV, respectively, that has been observed in young children.

Next, to evaluate boosting potency of WPV and SV, we focused on HI antibody titers in the sera obtained on day 49 (Figure 2). Notably, both WPV and SV were able to boost the levels of HI antibodies in WPV-primed macaques after the second vaccination. The HI antibody titers against influenza B virus vaccine strains also showed a similar tendency, but the titers were lower than those against influenza A virus vaccine strains. One of the reasons may be that the inactivation method applied to all four strains of viruses in the vaccine under the current regulations may be suitable for influenza A viruses but not for influenza B viruses in terms of maintaining antigenicity. Importantly, even after the second SV vaccination of macaques previously immunized with SV, no increase of HI antibody titers was observed, again indicating that the first SV vaccination had not primed the HI antibody response in the macaques. The results suggest that SV can only induce HI antibody responses in primed animals.

To confirm the boosting potency of SV, neutralizing antibody titers against influenza A virus vaccine strains were examined by micro-neutralization ELISA assays (Supplemental Figure 1). As expected, SV could induce neutralizing antibody response in animals previously inoculated with WPV but not with SV. Consistent with the HI antibody responses, even one inoculation of WPV induced substantial levels of neutralizing antibody and the titers were further elevated by the second inoculation with either WPV or SV. These results indicate that SV cannot prime naïve macaques effectively but only boost primed macaques, which is consistent with the observation from the previously conducted human clinical trial [16]. On the other hand, WPV can prime naïve macaques and boost primed macaques. Since the potency of vaccines to induce priming responses is indispensable when naïve individuals acquire protective immunity, these data indicate that WPV would be more suitable for naïve populations, such as young children.

3.2 Viral RNA in WPV effectively induces dendritic cell maturation.

To investigate the mechanistic basis for the differences in priming potency between WPV and SV, we next carried out *in vitro* experiments to determine whether differences in the handling of the vaccine antigens by antigen presenting cells (APCs) could account for this observation. Activation of APCs, such as macrophages and DC, in response to foreign antigens is triggered by the engagement of APC-expressed pattern recognition receptors

(PRRs) and results in secretion of proinflammatory cytokines and chemokines. To investigate whether WPV and SV could activate APC, key proinflammatory cytokines IL-6, TNF-α, and IFN-γ and the chemokine MIP-1α were evaluated in *in vitro* cultures of macaque splenic APC exposed to the vaccines (Figure 3). Since the isolation of cynomolgus macaque DCs was not reproducible in our system, $CD14^+$ monocytes from spleen were used as APCs. The remaining CD14-depleted splenocytes were also used as a DC-containing mixed cell population. Both populations were incubated for 6 hr with or without stimulants (either 1 mg/ml of LPS as positive control or the vaccine preparations containing 3 μg/ml HA), then culture supernatants were harvested and the concentrations of cytokines measured. In CD14-depleted splenocytes, concentrations of IL-6, TNF-α, MIP-1α, and IFN-γ were higher in WPV-treated cells than those in untreated and SV-treated cells. $CD14^+$ splenocytes responded strongly to LPS and produced IL-6, TNF-α, and MIP-1α, but WPV induced only IL-6. In contrast, SV failed to stimulate either CD14-depleted splenocytes or $CD14^+$ monocytes. IFN-γ was greatly induced by WPV in CD14-depleted splenocytes which contained DCs. These results suggest that WPV is a much more powerful activator of APC than is SV.

DC are the APC involved in presenting processed antigen to naïve T helper cells for the initial priming of these T cells to endow them with the capacity to provide "help" to B cells for the production of antibodies [19]. To study DC in more detail, analyses were performed using a single population of mouse splenic DCs. These were exposed to monovalent vaccines of A/California/07/2009 (H1N1) to simplify the interpretation. The DCs were stimulated with WPV or SV for 24 hr and induction of cytokines IL-6, TNF-α, IFN-γ, and chemokines MCP-1 and IP-10 was evaluated (Figure 4). As expected, WPV induced significantly higher levels of those cytokines than did SV and a PBS control. Since type-I IFNs are also typical innate immune products induced by activated DC, the mRNA levels of IFN-α and IFN-β as well as IP-10 in the DCs at 6 hr post-stimulation were also evaluated using quantitative-PCR (Figure 5). Compared with PBS, WPV induced almost 40-fold higher expression level of IP-10 mRNA, whereas SV induced barely detectable levels. In addition to mRNA of IP-10, mRNA levels of IFN-α and IFN-β were drastically elevated approximately 170- and 160-fold in DCs stimulated with WPV, respectively. SV did not transcribe mRNA of type-I IFNs in the DCs at all. Together these data indicate that WPV, but not SV, induced type-I IFNs as well as inflammatory cytokine and chemokine production from DC indicative of a much more potent activation and maturation of DC by WPV than SV.

Influenza viral RNA is a potent innate immune activator that can interact with the PRRs of DC, including Toll-like receptors (TLRs) and retinoic acid-inducible gene-I (RIG-I) like receptors (RLRs) [20-22] resulting in DC maturation and production of inflammatory cytokines and chemokines, especially type-I IFNs. Due to the different composition of WPV and SV it is likely that the characteristics of viral RNA contained in vaccines may differ. To investigate this, the RNA content in WPV and SV was compared by quantifying the RNA concentrations of each vaccine, which were calculated by the absorbance at 260 nm. Both vaccines contained equivalent amounts of viral RNA (Figure 6a), which is not surprising because they were prepared from the same virus suspension with or without an ether-disruption step. However, although these vaccines contain viral RNA at similar levels, the absorbance measurement does not distinguish viral RNA with the lengths or base-paired

structures that stimulate PRRs from degraded nucleotide fragments [23-27]. To detect viral RNA of a length recognizable by PRRs, quantitative-PCR was performed, targeting an 110 bp sequence in the influenza NP gene segment (Figure 6b). The copy number of the NP gene segment in WPV was 6.28 x 10^7 RNA copies in 1 ng total RNA, while that in SV was only 5.34 x 10^5 RNA copies in 1 ng total RNA. Therefore, WPV was considered to be over 100-fold richer in viral RNA with the length longer than 110 bp, compared with that in SV. Furthermore, as the PRRs that recognize viral RNA are intracellular, it was examined whether viral RNA in the vaccine preparations is actually taken up into DCs (Figure 6c). After the DCs were incubated with WPV or SV for an hr, unincorporated free RNA was removed by washing with PBS extensively, then total RNA was extracted from the cells for quantitative-PCR. The copy number of NP segments incorporated into 10^5 DCs was 5.77 x 10^5 after the treatment with WPV but only 634 RNA copies after treatment with SV. Since the amount of viral RNA of appropriate length contained in WPV was approximately 100 times more than that in SV, it is considered that the uptake of viral RNA contained in WPV is 10 times more efficient even if input RNA amount was the same. *In situ* hybridization of the NP gene segment further confirmed that viral RNA from WPV was actually incorporated into DCs (Supplemental Figure 2). While viral RNA signals in DCs incubated with SV randomly diffused through a viewing field, the signals in DCs incubated with WPV were localized in areas close to the nuclei. It is noted that input copy number of viral RNA in SV was adjusted to the same level as that in WPV treatment in this experiment. Similar perinuclear localization of the viral RNA signals was observed in DCs infected with influenza virus. Although this *in situ* hybridization data support the difference in RNA uptake efficiency, higher resolution analysis is needed to clarify the exact localization of RNA. Taken together, this effective delivery of viral RNA into DCs may explain a reason why WPV but not SV greatly stimulates innate responses in spleen-derived immune cells, which lead to the activation and maturation of DCs.

To examine whether WPV stimulates DCs *in vivo*, inguinal lymph nodes were collected from vaccinated mice at 6, 12, 24, and 48 hr post-vaccination and the surface expression level of CD86, a marker for mature DC, was analyzed using a flow cytometer (Figure 7 and Supplemental Figure 3). In addition to conventional DCs (cDCs), plasmacytoid DCs (pDCs) were analyzed. This subset of DC is known to be a potent inducer of IFN-α in response to viral RNA recognition by TLR7 [28-30]. The CD86 expression of cDCs in lymph nodes sampled at 24 and 48 hr after vaccination with WPV, was much greater than after vaccination with SV. The pDC from WPV-injected mice also expressed higher levels of CD86 than those from SV-inoculated mice at 12 hr post-vaccination. Greater expression of CD86 on DCs from WPV-vaccinated mice implied that WPV activates innate immunity and promotes DC maturation to enhance the antigen presentation potency for effective priming *in vivo*. Given that WPV delivered greater amounts of viral RNA into DCs as demonstrated by *in vitro* experiments, the activation of APCs by the viral RNA contained in WPV provides an explanation for its effective priming potency in mice and macaques.

3.3 WPV induced a significant antibody response at low doses.

A dose-sparing experiment using macaques was conducted to investigate any advantage of WPV in addition to the priming potency (Figure 8). Eight naïve cynomolgus

macaques were vaccinated twice with the various doses (full, 1/2, 1/4, or 1/8 doses) of quadrivalent WPV with a 4-week interval between injections. The full dose contained 15 μg HA per strain, the same amount as the commercially available seasonal influenza split vaccines. Plasma samples were periodically collected on day 0, 28, and 49 to evaluate antibody responses against the vaccine strains. HI antibody titers against influenza A virus vaccine strains on day 49 were significantly increased from day 0 or day 28 in all groups of monkeys. HI antibody titers against influenza B virus vaccine strains on day 49 increased significantly from day 0 or day 28 in macaques vaccinated with full or 1/2 doses of WPV, but not in monkeys vaccinated with 1/4 and 1/8 doses. The titres of HI antibody responses to influenza B virus vaccine strains were modest compared to those to influenza A virus vaccine strains, consistent with the data shown in Figure 2. Plasma samples were also tested in micro-neutralization ELISA assays and the results were in accord with the data of HI assay (Supplemental Figure 4). The boosting effect of the second vaccination seems to be fully achieved by even half the dose of WPV. The present results suggest that the full dose of WPV is not necessary for the boosting effect, thus the amount of vaccine could be reduced to half that of current seasonal influenza SVs.

4. Discussion

In this study we demonstrated the relative inefficiency of SV compared to WPV in priming a protective antibody response and provide evidence that this difference is due to inferior induction of innate immune mechanisms, most importantly the maturation of DCs. In contrast, SV exhibits comparative effectiveness to WPV in boosting immunity in macaques previously primed by WPV. These data are consistent with the observation in humans that current SV only provides adequate immunity in primed populations such as most adults but does not induce sufficient immune responses in unprimed populations [14, 16].

Historically, when SV were developed, these replaced WPV in spite of the impaired immunogenicity in young children because of the emphasis on WPV-associated adverse reactions such as fever [12, 13]. However, these side reactions, with the exception of those caused by egg-derived contaminants and residual formalin, can be indicative of well-functioning host immune responses, particularly the innate immune system [31, 32]. This is consistent with the present results where WPV, but not SV at a comparable antigen dose, induced innate immune responses as shown by the induction of cytokines and chemokines. Among them, inflammatory cytokines such as IL-6, IL-1, and TNF-α, as well as type-I IFNs, trigger febrile responses [31, 32]. Concurrently, the cytokines induced by signaling cascades of PRRs, such as TLRs and RLRs, play important roles in activation and maturation of DCs, leading to the induction of effective adaptive immunity. Thus, the innate immune system, including inflammatory cytokines, is tightly linked to the formation of robust adaptive immunity. This double-edged sword action of cytokines was only revealed in the 1990s and later, so at the time when WPV was replaced by SV because of the emphasis on the undesired pyrogenic reactions, the accompanying benefits from WPV-induced innate immunity were not understood nor properly evaluated.

Here we showed that recognition of viral RNA by PRRs on DC may be responsible for the differences in the ability of the vaccines to mount a primary response. The RNA

recognized by PRRs includes replication products and viral RNA structure; e.g. double- and single-stranded RNA, 5'-ppp RNA, and virus mRNA cap [33]. Given that activation of DCs through PRRs is necessary for DC maturation and subsequent adaptive immune responses and effective priming [34, 35], characteristics of viral RNA in vaccines are particularly important. Inactivated WPV does not replicate but viral RNA is retained within a virion and is able to efficiently trigger innate immune responses. Although SV also contains viral RNA, the amount of viral RNA detectable by qPCR in SV was only 1/100 of that in WPV as shown in Figure 6b. It was probably because the viral RNA in SV was degraded during storage and/or the manufacturing process involving disruption of the virion structure by ether and/or detergent. More importantly, the viral RNA is taken up by APCs such as DCs, to induce innate immune responses via PRRs located in the endosome or cytoplasm, not on the cell surface [36]. When the DCs were stimulated with WPV or SV containing the same HA protein concentration, the amount of viral RNA internalized to the cells was more than 1,000 times higher in WPV-stimulated cells compared with SV-stimulated ones (Figure 6c). Thus, this is the most likely reason for superiority of WPV both in innate and adaptive immunity in naïve animals, compared to SV. The differences in the potency to induce the "priming" between WPV and SV are schematically summarized in Supplemental Figure 5. After a WPV particle is captured, the entire component of the virion, including viral RNA, is incorporated into a DC. The virion structure is degraded in endosomes and released viral RNA is recognized by PRRs. Activation of DC through PRRs by the viral RNA induces DC maturation with up-regulation of MHC class I and II and costimulatory molecule CD80 and CD86 to enhance antigen presentation. After the WPV is endocytosed, digested and processed, antigenic epitopes are loaded onto MHC II molecules, which subsequently activate $CD4^+$ helper T cells. In addition, some antigens are directed to endolysosomes where they may gain access to the MHC I antigen processing pathway called the "cross-presentation pathway" in which, subsequently, antigenic epitopes are loaded onto MHC I molecules, and to activate $CD8^+$ cytotoxic T cells [37-40]. Importantly, WPV allows all epitopes of the structural proteins of a virus particle to be presented on MHC molecules. In fact, our previous study utilizing WPV and SV demonstrated the superiority of WPV over SV in terms of the induction of neutralizing antibodies and $CD8^+$ T cell responses in naïve mice [17]. Therefore, WPV induce stronger and broader humoral and cellular adaptive immunity in vaccinated individuals. On the other hand, in SV, the HA proteins that bind cellular sialic acid receptor are incorporated into DC, and the other viral proteins, particularly internal proteins and viral RNA, are not preferably taken up by APCs including DCs, resulting in inadequate DC maturation. As a result, SV does not effectively prime naïve populations. However, the addition of adjuvant to SV is one way to compensate for an ability to effectively activate immune response in naïve populations [41, 42]. In contrast to priming responses, DCs are not necessary for boosting responses, but rather the only interaction between memory B cells and memory T follicular helper cells is sufficient [43, 44]. As shown in Figure 2, SV boosted the primed macaques. However, it has been reported that WPV, but not SV, induces T cell-independent antibody responses in the boosting responses, resulting in faster recall of the memory response [45]. Although the present study did not confirm the superiority of WPV over SV in the boosting responses, it is now clear that WPV has advantages in the boosting as well as the priming response.

Since school-age children are one of the key spreaders for influenza in a community, immunization of children is essential to achieve "herd immunity" [7-10]. Herd immunity is a basic concept for epidemic control and an effective vaccine is the key to achieving this state of population immunity. With our findings, it seems difficult that herd immunity could be achieved using current split vaccines due to lack of priming potency. SV may still effectively work for people who are primed to influenza virus, but development of other types of vaccines to induce enough protective immune responses against influenza in children is an urgent task. Our new WPV is expected to immunize young children effectively and not to cause undesired reactions, at least those caused by egg-derived contaminants, due to the contribution of improved virus purification methods. Therefore, the present results prompt this project to clinical trials especially with young children. Comparing vaccine efficacy of WPV to SV in adults and children will provide valuable and new insights into the benefits of WPV. In addition, the dose-sparing experiments using macaques indicate that vaccination with even half dose of WPV is sufficient to induce protective immunity, probably with limited induction of inflammatory responses as reported previously [17]. This dose reduction is also an additional advantage for raising production capacity as well as lowering costs. Thus, this new WPV should be an alternative option for seasonal influenza vaccines, especially for children, because of effective immunogenicity in naïve individuals. In addition, WPV should be ideal to control pandemic influenza, a situation where all individuals are naïve to the causative agent. In both these contexts, we envisage that use of WPV would contribute significantly to global health.

Acknowledgments

We thank Mayumi Sasada, Mamiko Kawahara, and Hideaki Ishida for helping with experiments and all member of all Japan influenza vaccine study group for helpful discussion. We also thank Dr. Watanabe (National Institute of Infectious Disease in Japan) for kindly providing influenza virus strains, A/California/7/2009 (X-179A) (H1N1) pdm09, A/Singapore/GP1908/2015 (IVR-180) (H1N1), A/Hong Kong/4801/2014 (X-263) (H3N2), B/Phuket /3073/2013 (Yamagata linage), and B/Texas/2/2013 (Victoria lineage). The project was supported by the Japan Initiative for Global Research Network on Infectious Diseases (J-GRID; JP19fm0108008), the Japan Program for Infectious Diseases Research and Infrastructure (JIDRI; JP20wm0125008) and Research Program on Emerging and Re-emerging Infectious Diseases (21fk0108142) from Japan Agency for Medical Research and Development (AMED), the Global Institution for Collaborative Research and Education (GI-CoRE) program of Hokkaido University, the Japan International Cooperation Agency (JICA) program, the Program for Leading Graduate Schools (F01) from the Japan Society for the Promotion of Science (JSPS) and Doctoral Program for World-leading Innovative & Smart Education (WISE) Program (1801) from the Ministry of Education, Culture, Sports, Science and Technology (MEXT). M Ohno and M Shingai were supported by grants from JSPS KAKENHI (grant numbers 17K15367 and 18K07135, respectively). C Handabile was supported by WISE Program (1801), MEXT. K Kedzierska was supported by the NHMRC Leadership Investigator Grant (#1173871)

Figure legends

Figure 1

Protective immune responses induced in mice vaccinated with WPV.

C57BL/6 mice (n =5 per group) were inoculated subcutaneously with PBS, SV (3 μg HA), or various doses of WPV (3–0.12 μg HA). On day 28 after vaccination, the mice were challenged intranasally with a lethal dose (3,000 PFU in 40 μl PBS) of A/Singapore/2015 (H1N1) virus. Mice were euthanized at 5 days post-infection (dpi) and lungs harvested for plaque assay (a). The body weight of the mice was monitored daily until 5 dpi (b). Data are expressed as the percentage of the starting weight on day 0 and symbols represent the mean and SEM of the group. To measure the neutralizing antibody titers induced by vaccines, sera were collected on day 24 after vaccination prior to challenge (c). Box plots in (a) and (c) indicate the median (line in box), the interquartile range (ends of box), and whiskers from min to max. Statistical analysis was performed using two-way ANOVA with multiple comparisons. *$p < 0.05$, **$p < 0.01$, ***$p < 0.001$.

Figure 2

Hemagglutination inhibiting antibodies induced after vaccination of naïve macaques

Cynomolgus macaques (n=4 per group) were vaccinated twice by the subcutaneous route with either WPV or SV (prime and boost) as indicated. Serum samples were collected from each animal on day 0, 28, and 49 and assayed for hemagglutination inhibiting antibodies against vaccine strains, A/Singapore/ 2015 (H1N1) (a), A/Hong Kong/2014 (H3N2) (b), B/Phuket /2013 (Yamagata linage) (c), or B/Texas/2013 (Victoria lineage) (d). Box plots indicate the median (line in box), the interquartile range (ends of box), and whiskers from min to max. Statistical analysis was performed using two-way ANOVA with multiple comparisons. *$p < 0.05$, **$p < 0.01$, ***$p < 0.001$.

Figure 3

Cytokine production in macaque $CD14^+$ and $CD14^-$ splenocytes cultured with the vaccines

$CD14^+$ and CD14-depleted splenocytes collected from unimmunized cynomolgus macaques were cultured with WPV, SP, or LPS for 6 hr. Concentrations of IL-6 (a), TNF-α (b), MIP-1α (c), and INF-γ (d) in the supernatants were measured. The results shown are representative of two independent experiments.

Figure 4

Vaccine-induced cytokine production in mouse DCs

DCs collected from mice were incubated in the presence of PBS, WPV (5μg of HA), or SV (5μg of HA) for 24 hr and culture supernatants were collected for measurement of the cytokines and chemokines IL-6 (a), TNF-α (b), MCP-1 (c), IFN-γ (d), and IP-10 (e). Each bar represents the mean ± SEM of 3 replicates. In each panel, black bars indicate the amount of cytokine induced from cells treated with PBS, light gray bars indicate the amount of cytokine induced from WPV-stimulated cells, and dark gray bars indicate the amount of

cytokine induced from SV-stimulated cells. Statistical analysis was performed using one-way ANOVA with multiple comparisons. *$p < 0.05$, **$p < 0.01$.

Figure 5

Type-I IFN induction in mouse DCs stimulated with the vaccines

One hundred thousand DCs from mouse spleen were cultured with WPV, SV, or PBS for 6 hr. The mRNA expression levels of IP-10 (a), IFN-α (b) and IFN-β (c) in DCs were analyzed using qPCR. Each bar represents the mean ± SEM of triplicate samples and the data shown are representative of three independent experiments. Statistical analysis was performed using one-way ANOVA with multiple comparisons. ***$p < 0.001$.

Figure 6

Levels of viral RNA in vaccine preparations and its uptake into DCs

The concentration of RNA extracted from 5μg HA of WPV or SV was calculated from the absorbance at 260 nm (a). The copy number of 110 bp sequence of the influenza virus NP segment in the extracted RNA was determined using qPCR (b). One hundred thousand DCs were incubated with WPV or SV for an hr. After removal of residual RNA by extensive washing with PBS, intracellular RNA was extracted and the copy number of the NP segment in DCs determined using qPCR (c). Each bar represents the mean ± SEM of triplicate samples and the data shown are representative of three independent experiments. Statistical analysis was performed using unpaired *t*-test. ***$p < 0.001$.

Figure 7

Surface expression of the maturation marker CD86 on DCs from vaccinated mice

Mice were vaccinated with WPV or SV and lymph nodes were collected at 6, 12, 24, and 48 hr post vaccination. The inguinal lymph nodes collected from five mice were combined and used for data analysis at each point. CD86 expression on conventional DCs (cDC) (a) and plasmacytoid DCs (pDCs) (b) in the lymph nodes was analyzed by flow cytometry. Expression levels of CD86 are shown as mean fluorescence intensity (MFI). cDCs were identified as the CD19 negative, CD11b positive, CD11c positive, and B220 negative population, while pDCs were CD19 negative, CD11b negative, CD11c positive, and B220 positive.

Figure 8

The relationship between WPV dose and hemagglutination inhibition titers in macaques

Cynomolgus macaques (n=8 per group) were vaccinated twice, 4 weeks apart, with the indicated doses of WPV delivered subcutaneously. Serum samples were collected on day 0, 28, and 49 and hemagglutination inhibition titers against vaccine strains, A/Singapore/ 2015 (H1N1) (a), A/Hong Kong/2014 (H3N2) (b), B/Phuket /2013 (Yamagata linage) (c), or B/Texas/2013 (Victoria lineage) (d), were measured. Box plots indicate the median (line in box), the interquartile range (ends of box), and whiskers from min to max. Statistical analysis was performed using two-way ANOVA with multiple comparisons. *$p < 0.05$, **$p < 0.01$, ***$p < 0.001$.

Supplemental Figure 1

Neutralization titers in the serum of vaccinated macaques

Cynomolgus macaques (n=4 per group) were vaccinated twice, 4 weeks apart, by the subcutaneous route with either WPV or SV (prime and boost) as indicated. Serum samples were collected on day 0, 28, and 49 and serum neutralizing antibody titers against A/Singapore/2015 (H1N1) (a) or A/Hong Kong/2014 (H3N2) (b) were measured. Box plots indicate the median (line in box), the interquartile range (ends of box), and whiskers from min to max. Statistical analysis was performed using two-way ANOVA with multiple comparisons. *$p < 0.05$, **$p < 0.01$, ***$p < 0.001$.

Supplemental Figure 2

Incorporated viral RNA in DCs detected using *in situ* hybridization

The mouse DCs were cultured overnight on tissue culture slides. The attached DCs on slide were incubated for 3 hr with WPV or SV, each of which had been adjusted to 5×10^5 copies of the NP segment. As a positive control, live virus at MOI = 10 was used. The NP segment incorporated into the DCs was detected by *in situ* hybridization. In these representative images, green or blue color indicate specific signal to NP segment or cell nuclei, respectively. Long arrows indicate NP segments in the DCs. Short arrow indicates aggregated NP segments.

Supplemental Figure 3

Gating Strategy and CD86 expression on cDCs and pDCs from vaccinated mice

Mice were vaccinated with WPV or SV and lymph nodes were collected at 6, 12, 24, and 48 hr post vaccination. The inguinal lymph nodes collected from five mice were combined and used for data analysis at each point. Representative gating strategy for FACS analysis is shown in (a); CD11b-positive/B220-negative and CD11b-negative/B220-positive populations in CD19-negative/CD11c-positive populations are determined as cDCs and pDCs, respectively. The CD86 expression on cDCs and pDCs at each time point was shown in (b); Surface expression of CD86 on cDCs and pDCs was compared between WPV vaccinated (red-lined histograms) and SV vaccinated mice (blue-filled histograms). Gray-filled and black-lined histograms represent matched isotype controls for cDCs and pDCs in mice vaccinated with WPV and SV vaccines.

Supplemental Figure 4

Neutralization titers after two inoculations of reduced doses of WPV in macaques

Cynomolgus macaques (n=8 per group) were vaccinated twice, 4 weeks apart, with the indicated doses of WPV. Serum samples were collected on day 0, 28, and 49 and neutralization titers against A/Singapore/ 2015 (H1N1) (a) or A/Hong Kong/2014 (H3N2) (b) were measured. Box plots indicate the median (line in box), the interquartile range (ends of box), and whiskers from min to max. Statistical analysis was performed using two-way ANOVA with multiple comparisons. *$p < 0.05$, **$p < 0.01$, ***$p < 0.001$.

Supplemental Figure 5

The differences in the potency to induce DC maturation between WPV and SV

Schematic representation of the expected mechanism of DC maturation and antigen presentation by WPV and SV is shown. Upon capturing a WPV particle, the entire component of the virion, including viral RNA, is incorporated into a DC. Viral RNA is released from the virion and stimulates a PRR signaling cascade, leading to the DC maturation with up-regulation of MHC class I/II and CD80/86. In contrast, although HA proteins of SV bind cellular sialic acid and are incorporated into a DC, other viral components, particularly viral RNA, are not effectively taken into the cell, resulting in inadequate DC maturation. MHC, Major Histocompatibility Complex; TCR, T Cell Receptor.

References

[1] Lambert L, Fauci A. CURRENT CONCEPTS Influenza Vaccines for the Future. New England Journal of Medicine. 2010;363:2036-44.

[2] Stohr K, Kieny M, Wood D. Influenza pandemic vaccines: how to ensure a low-cost, low-dose option. Nature Reviews Microbiology. 2006;4:565-6.

[3] Petrova V, Russell C. The evolution of seasonal influenza viruses. Nature Reviews Microbiology. 2018;16:47-60.

[4] Reber A, Chirkova T, Kim J, Cao W, Biber R, Shay D, et al. Immunosenescence and Challenges of Vaccination against Influenza in the Aging Population. Aging and Disease. 2012;3:68-90.

[5] Thompson W, Weintraub E, Dhankhar P, Cheng P, Brammer L, Meltzer M, et al. Estimates of US influenza-associated deaths made using four different methods. Influenza and Other Respiratory Viruses. 2009;3:37-49.

[6] Dorratoltaj N, Marathe A, Lewis B, Swarup S, Eubank S, Abbas K. Epidemiological and economic impact of pandemic influenza in Chicago: Priorities for vaccine interventions. Plos Computational Biology. 2017;13.

[7] Bell D, Nicoll A, Fukuda K, Horby P, Monto A, Grp WHOW. Nonpharmaceutical interventions for pandemic influenza, international measures. Emerging Infectious Diseases. 2006;12:81-7.

[8] Stevenson E, Barrios L, Cordell R, Delozier D, Gorman S, Koenig L, et al. Pandemic Influenza Planning: Addressing the Needs of Children. American Journal of Public Health. 2009;99:S255-S60.

[9] Principi N, Esposito S. Are we ready for universal influenza vaccination in paediatrics? Lancet Infectious Diseases. 2004;4:75-83.

[10] Principi N, Esposito S. Influenza vaccine use to protect healthy children: A debated topic. Vaccine. 2018;36:5391-6.

[11] Barberis I, Myles P, Ault S, Bragazzi N, Martini M. History and evolution of influenza control through vaccination: from the first monovalent vaccine to universal vaccines. J Prev Med Hyg. 2016;57:E115-E20.

[12] Nakayama T. An inflammatory response is essential for the development of adaptive immunity-immunogenicity and immunotoxicity. Vaccine. 2016;34:5815-8.

[13] Peck F. Purified influenza virus vaccine - A study of viral reactivity and antigenicity. Journal of the American Medical Association. 1968;206:2277-82.

[14] Parkman P, Hopps H, Rastogi S, Meyer H. Summary of clinical-trials of influenza-virus vaccines in adults. Journal of Infectious Diseases. 1977;136:S722-S30.

[15] Gross P, Ennis F. Influenza vaccine - split-product versus whole-virus types - How do they differ. New England Journal of Medicine. 1977;296:567-8.
[16] Gross P, Ennis F, Gaerlan P, Denson L, Denning C, Schiffman D. Controlled double-blind comparison of reactogenicity, immunogenicity, and protective efficacy of whole-virus and split-product influenza vaccines in children. Journal of Infectious Diseases. 1977;136:623-32.
[17] Sekiya T, Mifsud E, Ohno M, Nomura N, Sasada M, Fujikura D, et al. Inactivated whole virus particle vaccine with potent immunogenicity and limited IL-6 induction is ideal for influenza. Vaccine. 2019;37:2158-66.
[18] Kida H, Brown L, Webster R. Biological-activity of monoclonal-antibodies to operationally defined antigenic regions on the hemagglutinin molecule of A/Seal/Massachusetts/1/80 (H7N7) influenza-virus. Virology. 1982;122:38-47.
[19] Janeway Jr C. The priming of helper T cells. Semin Immunol. 1989;1:13-20.
[20] Diebold S, Kaisho T, Hemmi H, Akira S, Sousa C. Innate antiviral responses by means of TLR7-mediated recognition of single-stranded RNA. Science. 2004;303:1529-31.
[21] Lund J, Alexopoulou L, Sato A, Karow M, Adams N, Gale N, et al. Recognition of single-stranded RNA viruses by Toll-like receptor 7. Proceedings of the National Academy of Sciences of the United States of America. 2004;101:5598-603.
[22] Liu G, Park H, Pyo H, Liu Q, Zhou Y. Influenza A Virus Panhandle Structure Is Directly Involved in RIG-I Activation and Interferon Induction. Journal of Virology. 2015;89:6067-79.
[23] Baum A, Garcia-Sastre A. Preference of RIG-I for short viral RNA molecules in infected cells revealed by next-generation sequencing. Virulence. 2011;2:166-9.
[24] Kato H, Takeuchi O, Mikamo-Satoh E, Hirai R, Kawai T, Matsushita K, et al. Length-dependent recognition of double-stranded ribonucleic acids by retinoic acid-inducible gene-I and melanoma differentiation-associated gene 5. Journal of Experimental Medicine. 2008;205:1601-10.
[25] Schmidt A, Schwerd T, Hamm W, Hellmuth J, Cui S, Wenzel M, et al. 5 '-triphosphate RNA requires base-paired structures to activate antiviral signaling via RIG-I. Proceedings of the National Academy of Sciences of the United States of America. 2009;106:12067-72.
[26] Schlee M, Roth A, Hornung V, Hagmann C, Wimmenauer V, Barchet W, et al. Recognition of 5 ' Triphosphate by RIG-I Helicase Requires Short Blunt Double-Stranded RNA as Contained in Panhandle of Negative-Strand Virus. Immunity. 2009;31:25-34.
[27] Botos I, Liu L, Wang Y, Segal D, Davies D. The Toll-like receptor 3:dsRNA signaling complex. Biochimica Et Biophysica Acta-Gene Regulatory Mechanisms. 2009;1789:667-74.
[28] Cella M, Jarrossay D, Facchetti F, Alebardi O, Nakajima H, Lanzavecchia A, et al. Plasmacytoid monocytes migrate to inflamed lymph nodes and produce large amounts of type I interferon. Nature Medicine. 1999;5:919-23.
[29] Siegal F, Kadowaki N, Shodell M, Fitzgerald-Bocarsly P, Shah K, Ho S, et al. The nature of the principal type 1 interferon-producing cells in human blood. Science. 1999;284:1835-7.
[30] Kadowaki N, Antonenko S, Lau J, Liu Y. Natural interferon alpha/beta-producing cells link innate and adaptive immunity. Journal of Experimental Medicine. 2000;192:219-25.
[31] Evans S, Repasky E, Fisher D. Fever and the thermal regulation of immunity: the immune system feels the heat. Nature Reviews Immunology. 2015;15:335-49.
[32] Hasday J, Thompson C, Singh I. Fever, Immunity, and Molecular Adaptations. Comprehensive Physiology. 2014;4:109-48.
[33] Iwasaki A, Gottesman S, Harwood C, Schneewind O. A Virological View of Innate Immune Recognition. Annual Review of Microbiology, Vol 66. 2012;66:177-96.

[34] Steinman R, Hemmi H, Pulendran B, Ahmed R. Dendritic cells: Translating innate to adaptive immunity. From Innate Immunity To Immunololgical Memory. 2006;311:17-58.
[35] Pasare C, Medzhitov R, Gupta S, Paul W, Steinman R. Toll-like receptors: Linking innate and adaptive immunity. Mechanisms of Lymphocyte Activation and Immune Regulation X: Innate Immunity. 2005;560:11-8.
[36] Jensen S, Thomsen A. Sensing of RNA Viruses: a Review of Innate Immune Receptors Involved in Recognizing RNA Virus Invasion. Journal of Virology. 2012;86:2900-10.
[37] Ackerman A, Cresswell P. Cellular mechanisms governing cross-presentation of exogenous antigens. Nature Immunology. 2004;5:678-84.
[38] Amigorena S, Savina A. Intracellular mechanisms of antigen cross presentation in dendritic cells. Current Opinion in Immunology. 2010;22:109-17.
[39] Gromme M, Neefjes J. Antigen degradation or presentation by MHC class I molecules via classical and non-classical pathways. Molecular Immunology. 2002;39:181-202.
[40] Ramachandra L, Simmons D, Harding C. MHC molecules and microbial antigen processing in phagosomes. Current Opinion in Immunology. 2009;21:98-104.
[41] Lin Y, Wen C, Lin Y, Hsieh W, Chang C, Chen Y, et al. Oil-in-water emulsion adjuvants for pediatric influenza vaccines: a systematic review and meta-analysis. Nature Communications. 2020;11.
[42] Patel S, Bizjajeva S, Lindert K, Heijnen E, Oberye J. Cumulative clinical experience with MF59-adjuvanted trivalent seasonal influenza vaccine in young children. International Journal of Infectious Diseases. 2019;85:S26-S38.
[43] Ise W, Inoue T, McLachlan J, Kometani K, Kubo M, Okada T, et al. Memory B cells contribute to rapid Bcl6 expression by memory follicular helper T cells. Proceedings of the National Academy of Sciences of the United States of America. 2014;111:11792-7.
[44] Kurosaki T, Kometani K, Ise W. Memory B cells. Nature Reviews Immunology. 2015;15:149-59.
[45] Onodera T, Hosono A, Odagiri T, Tashiro M, Kaminogawa S, Okuno Y, et al. Whole-Virion Influenza Vaccine Recalls an Early Burst of High-Affinity Memory B Cell Response through TLR Signaling. Journal of Immunology. 2016;196:4172-84.

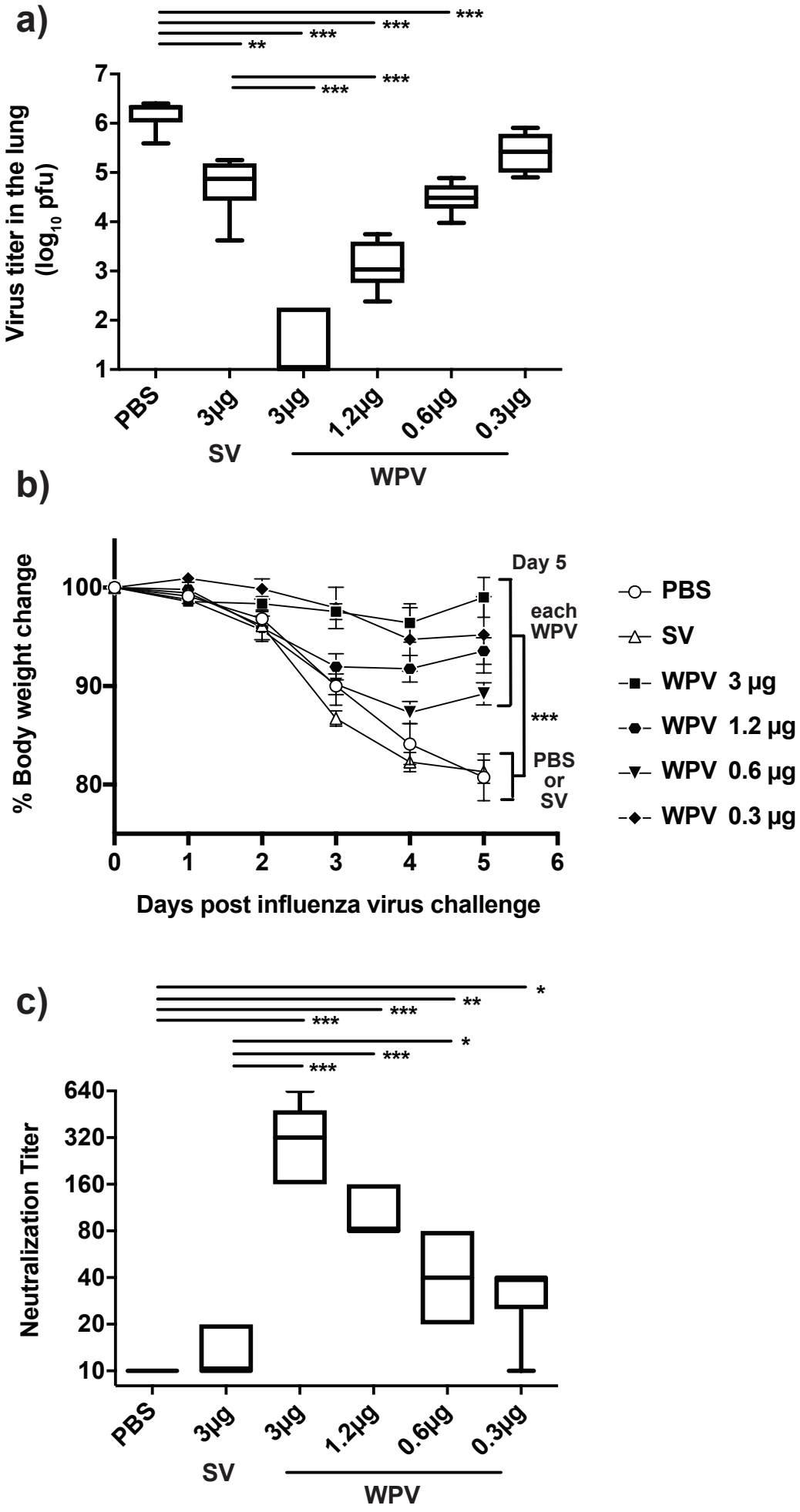
a)
***
***
***
**
***
***
Virus titer in the lung
(log10 pfu)
7
6
5
4
3
2
1
PBS
3µg
3µg
1.2µg
0.6µg
0.3µg
SV
WPV
b)
% Body weight change
100
90
80
Day 5
each WPV
***
PBS or SV
0
1
2
3
4
5
6
Days post influenza virus challenge
PBS
SV
WPV 3 µg
WPV 1.2 µg
WPV 0.6 µg
WPV 0.3 µg
c)
*
**
***
***
*
***
Neutralization Titer
640
320
160
80
40
20
10
PBS
3µg
3µg
1.2µg
0.6µg
0.3µg
SV
WPV

Figure 1

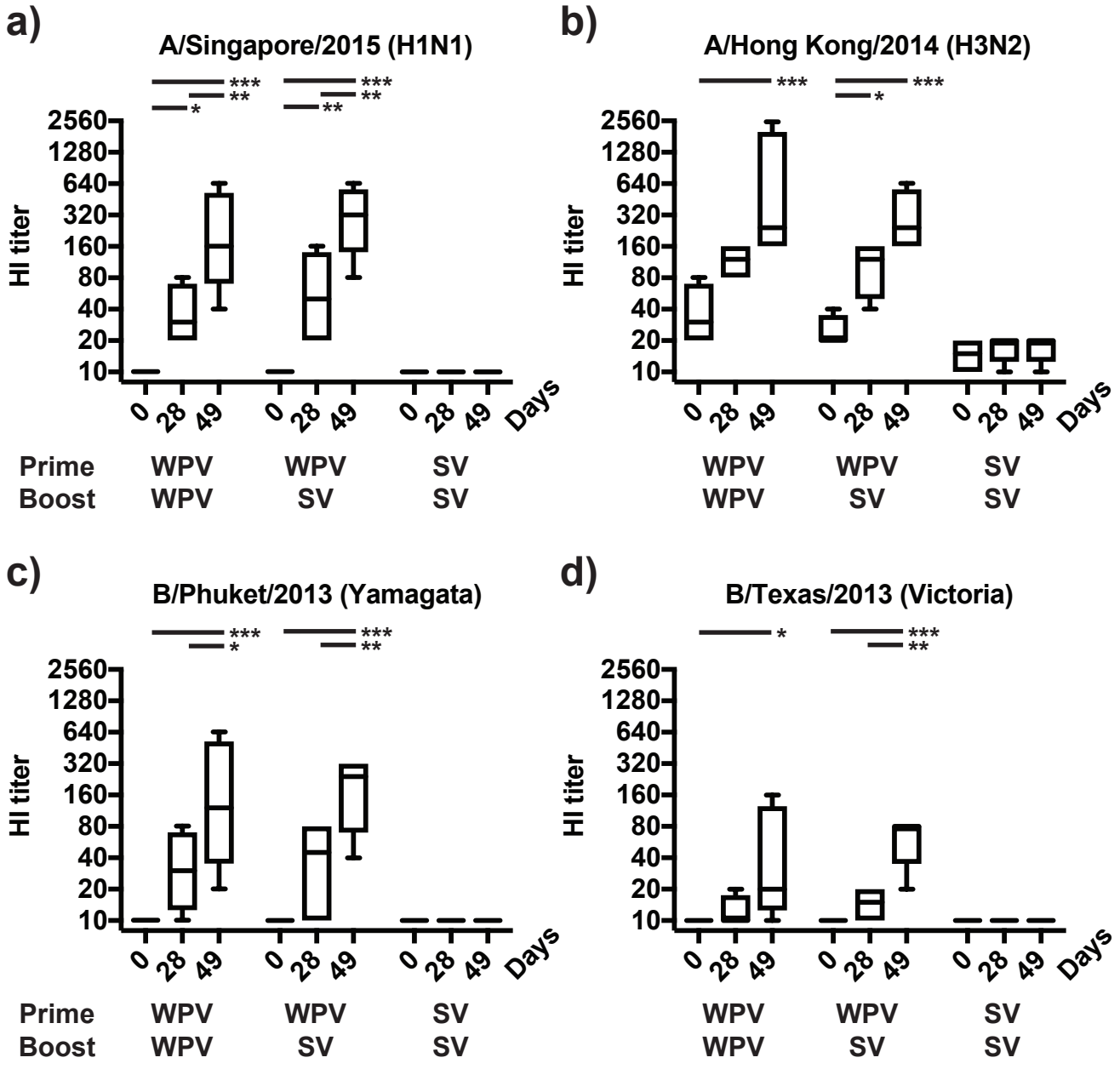
a)
A/Singapore/2015 (H1N1)
b)
A/Hong Kong/2014 (H3N2)
c)
B/Phuket/2013 (Yamagata)
d)
B/Texas/2013 (Victoria)
HI titer
2560
1280
640
320
160
80
40
20
10
0
28
49
Days
***
**
*
Prime
Boost
WPV
SV

Figure 2

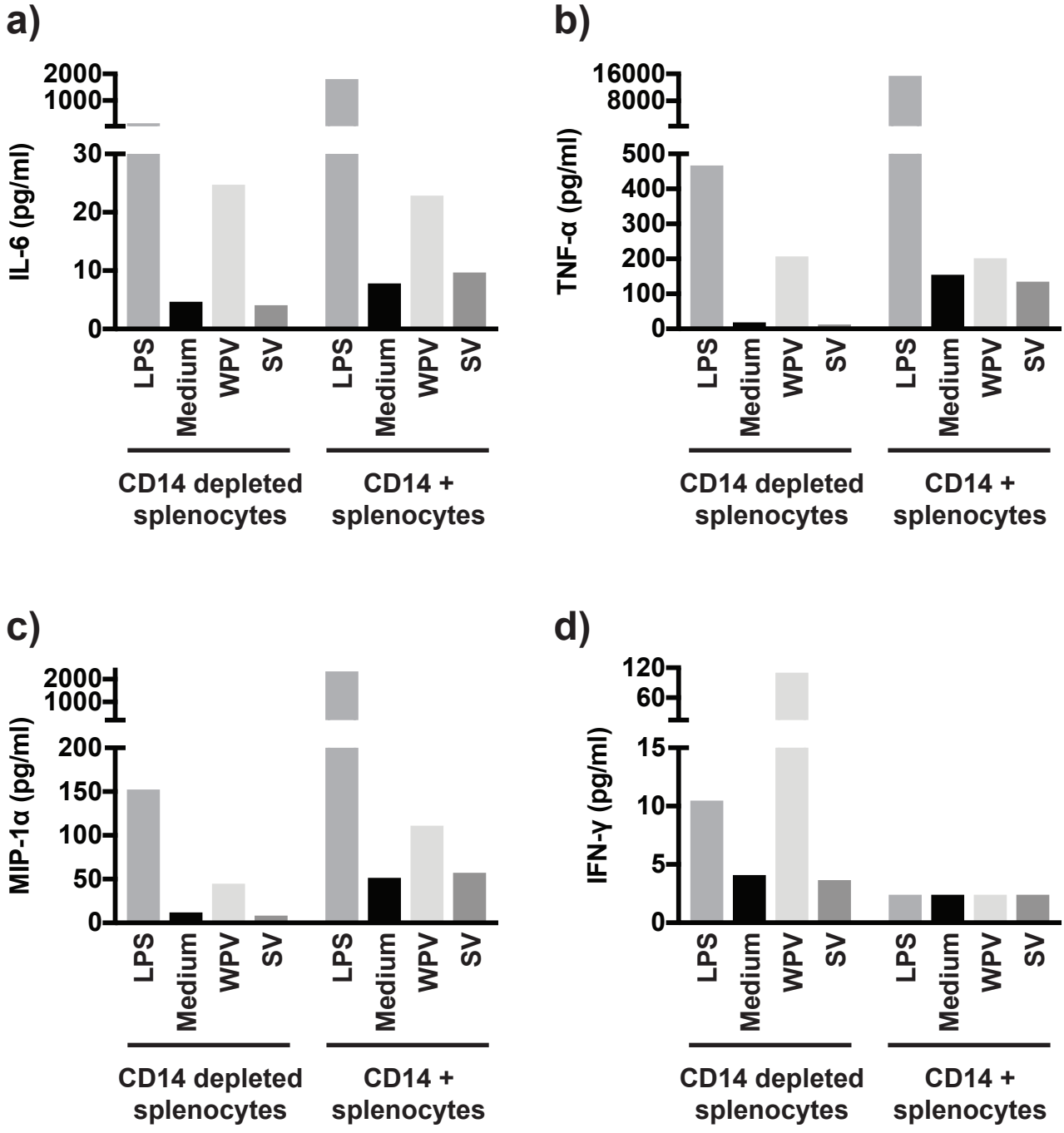
a)
2000
1000
30
20
10
0
IL-6 (pg/ml)
LPS
Medium
WPV
SV
LPS
Medium
WPV
SV
CD14 depleted splenocytes
CD14 + splenocytes
b)
16000
8000
500
400
300
200
100
0
TNF-α (pg/ml)
LPS
Medium
WPV
SV
LPS
Medium
WPV
SV
CD14 depleted splenocytes
CD14 + splenocytes
c)
2000
1000
200
150
100
50
0
MIP-1α (pg/ml)
LPS
Medium
WPV
SV
LPS
Medium
WPV
SV
CD14 depleted splenocytes
CD14 + splenocytes
d)
120
60
15
10
5
0
IFN-γ (pg/ml)
LPS
Medium
WPV
SV
LPS
Medium
WPV
SV
CD14 depleted splenocytes
CD14 + splenocytes

Figure 3

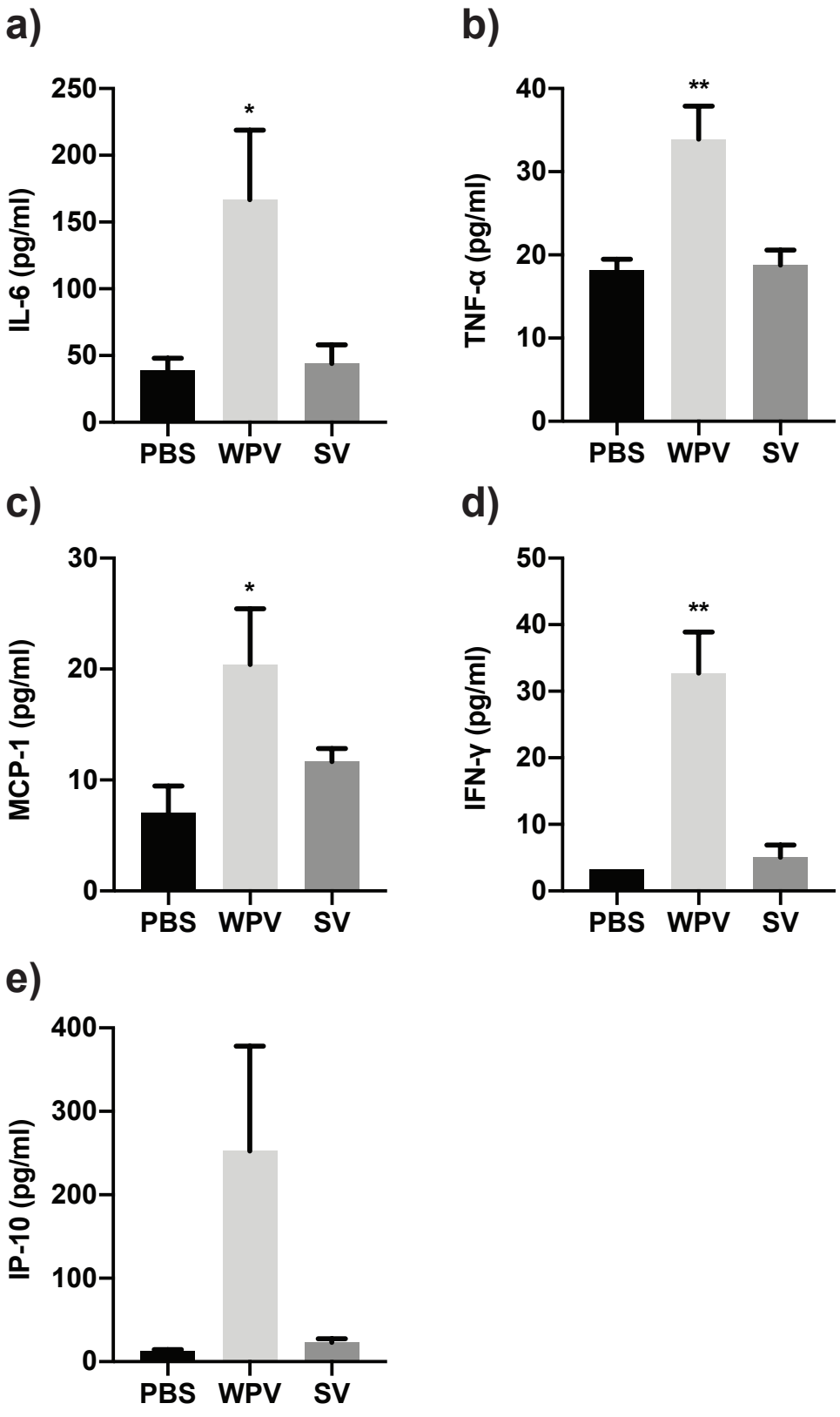
a)
IL-6 (pg/ml)
250
200
150
100
50
0
*
PBS
WPV
SV
b)
TNF-α (pg/ml)
40
30
20
10
0
**
PBS
WPV
SV
c)
MCP-1 (pg/ml)
30
20
10
0
*
PBS
WPV
SV
d)
IFN-γ (pg/ml)
50
40
30
20
10
0
**
PBS
WPV
SV
e)
IP-10 (pg/ml)
400
300
200
100
0
PBS
WPV
SV

Figure 4

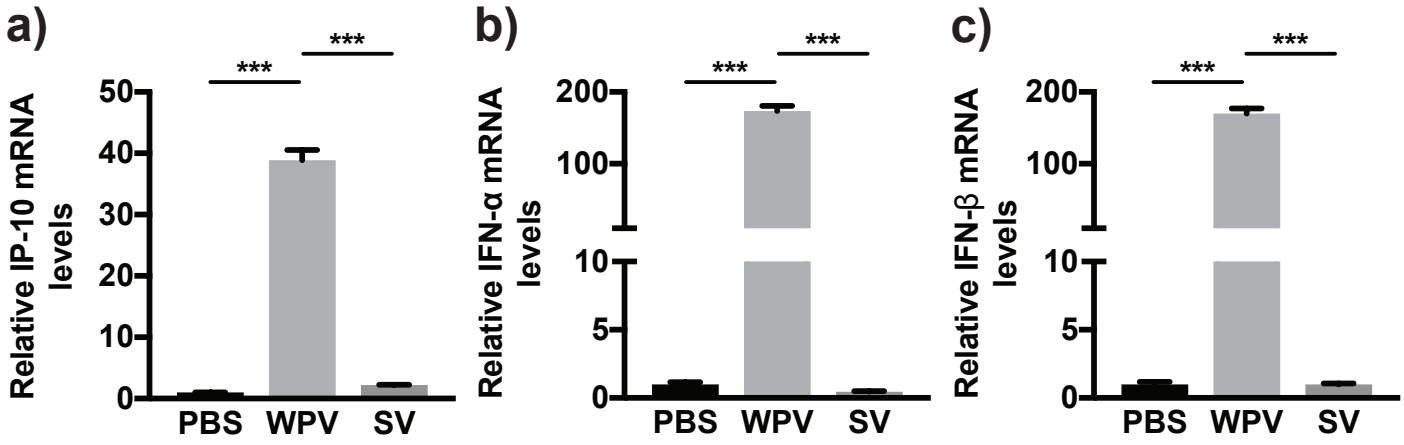
a)
Relative IP-10 mRNA levels
50
40
30
20
10
0
***
***
PBS
WPV
SV
b)
Relative IFN-α mRNA levels
200
100
10
5
0
***
***
PBS
WPV
SV
c)
Relative IFN-β mRNA levels
200
100
10
5
0
***
***
PBS
WPV
SV

Figure 5

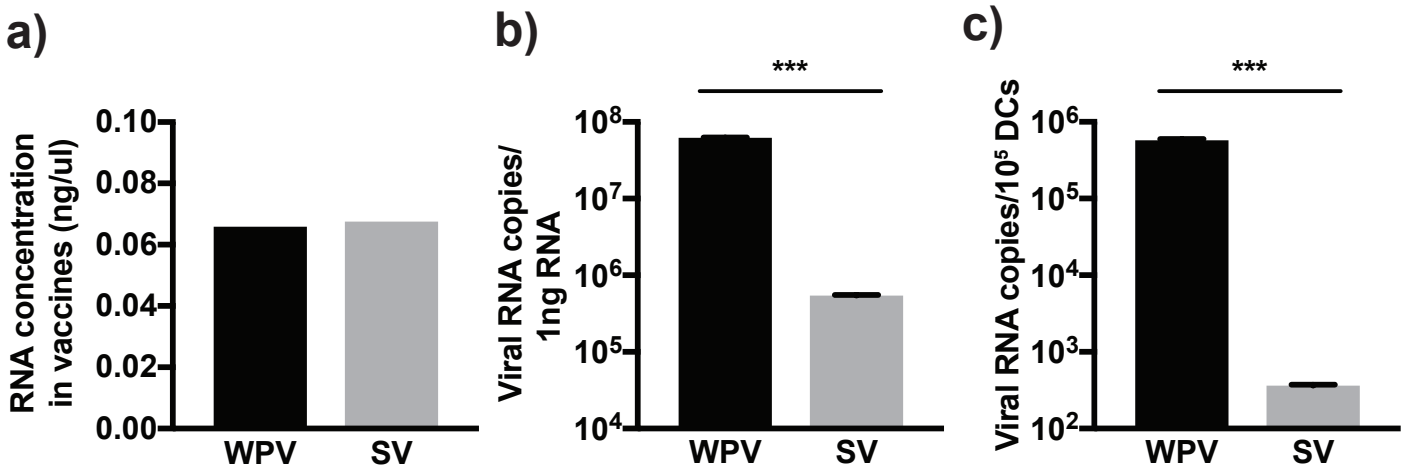
a)
RNA concentration in vaccines (ng/ul)
0.10
0.08
0.06
0.04
0.02
0.00
WPV
SV
b)
***
Viral RNA copies/ 1ng RNA
10^8
10^7
10^6
10^5
10^4
WPV
SV
c)
***
Viral RNA copies/10^5 DCs
10^6
10^5
10^4
10^3
10^2
WPV
SV

Figure 6

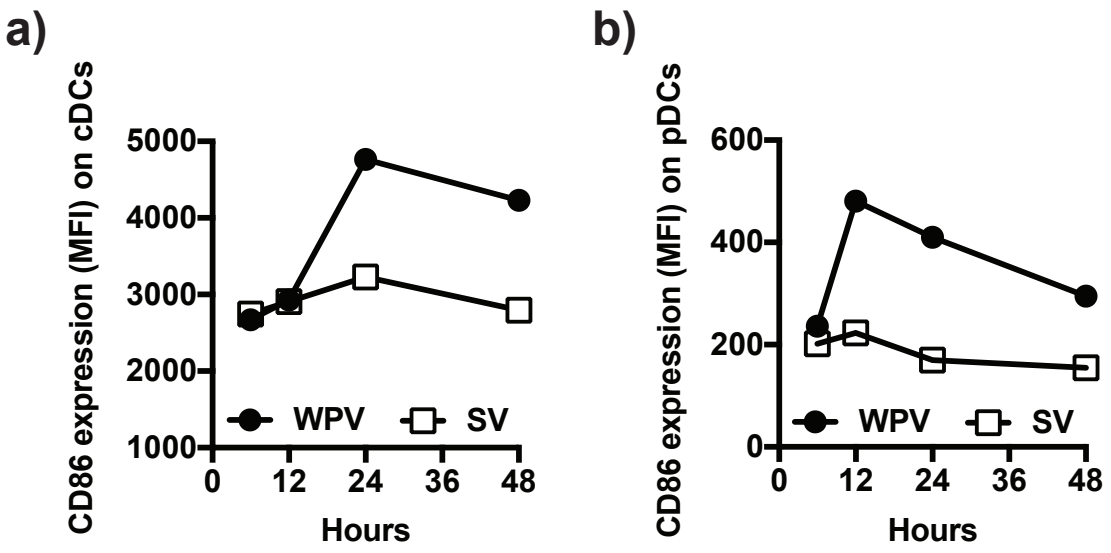
a)
CD86 expression (MFI) on cDCs
5000
4000
3000
2000
1000
0
12
24
36
48
Hours
WPV
SV
b)
CD86 expression (MFI) on pDCs
600
400
200
0
0
12
24
36
48
Hours
WPV
SV

Figure 7

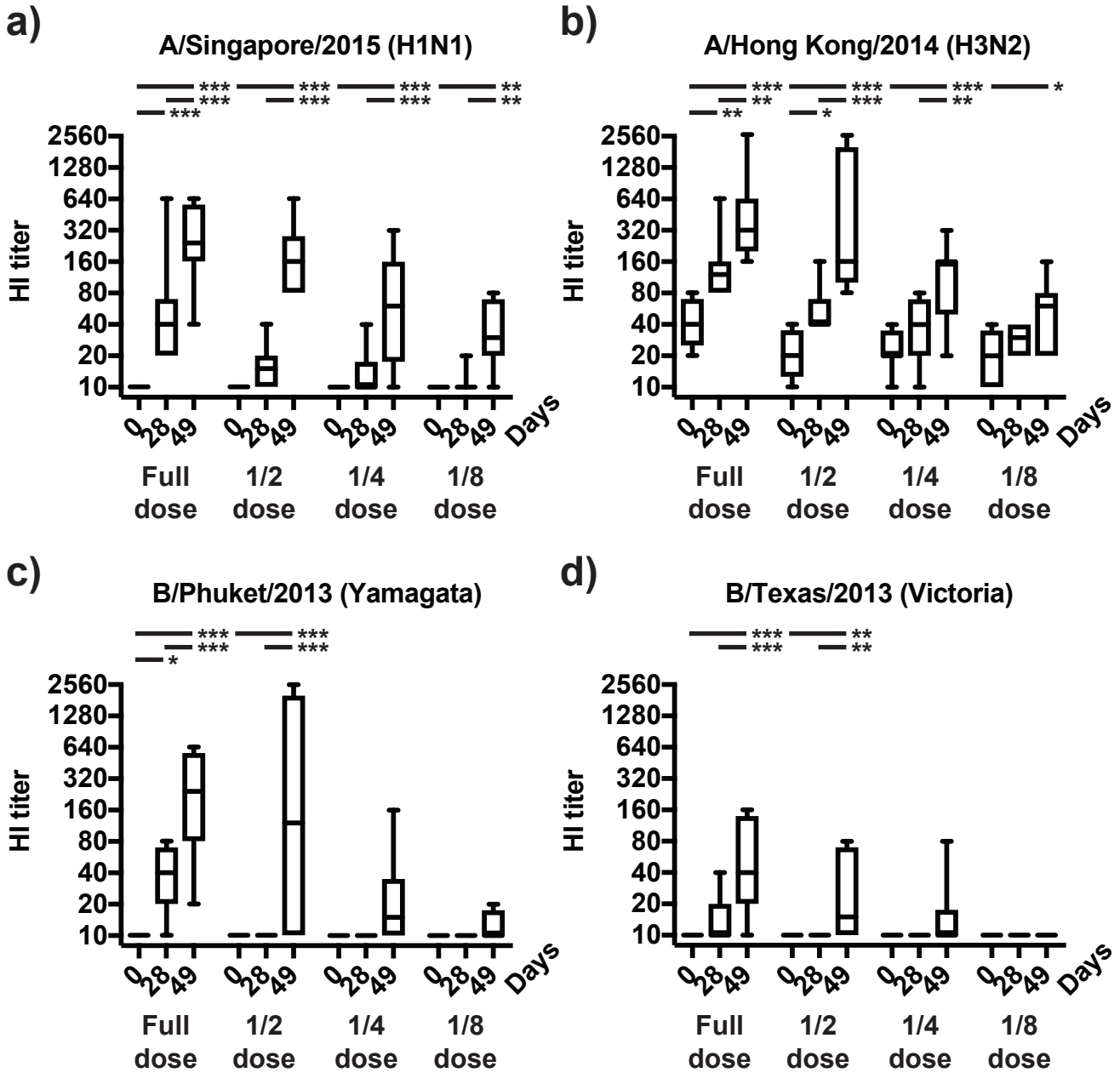
a)
A/Singapore/2015 (H1N1)
b)
A/Hong Kong/2014 (H3N2)
c)
B/Phuket/2013 (Yamagata)
d)
B/Texas/2013 (Victoria)
HI titer
2560
1280
640
320
160
80
40
20
10
0 28 49
Days
Full dose
1/2 dose
1/4 dose
1/8 dose

Figure 8

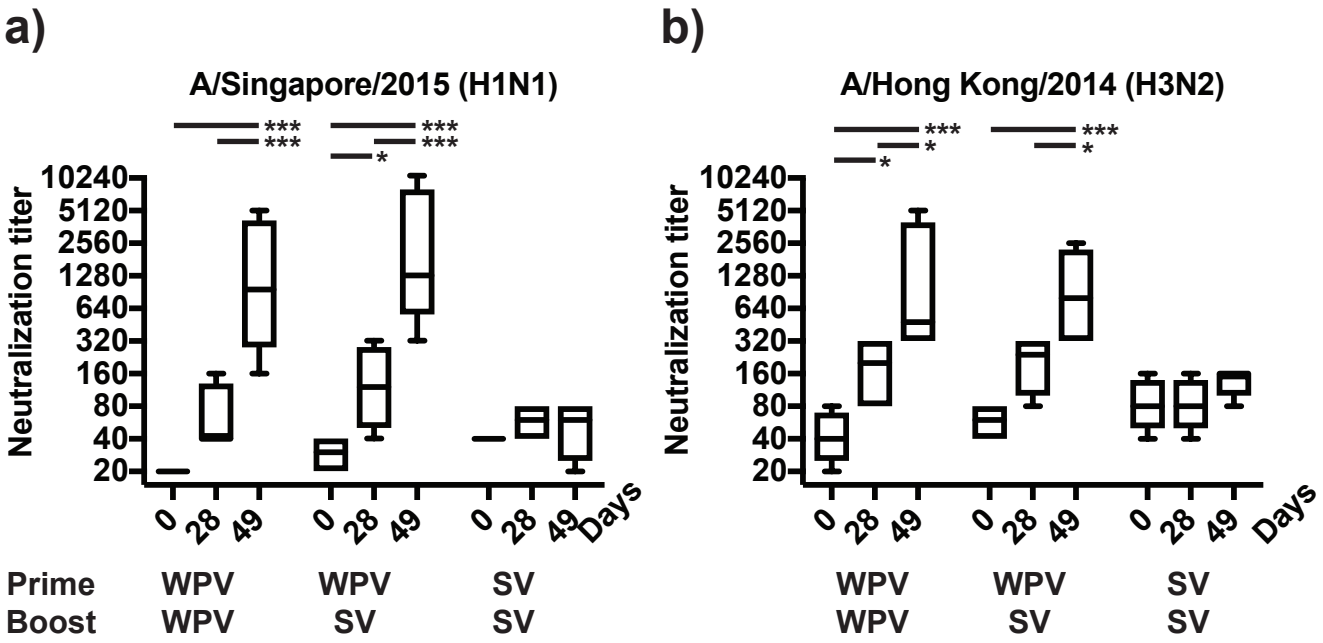

Supplimental Figure 1

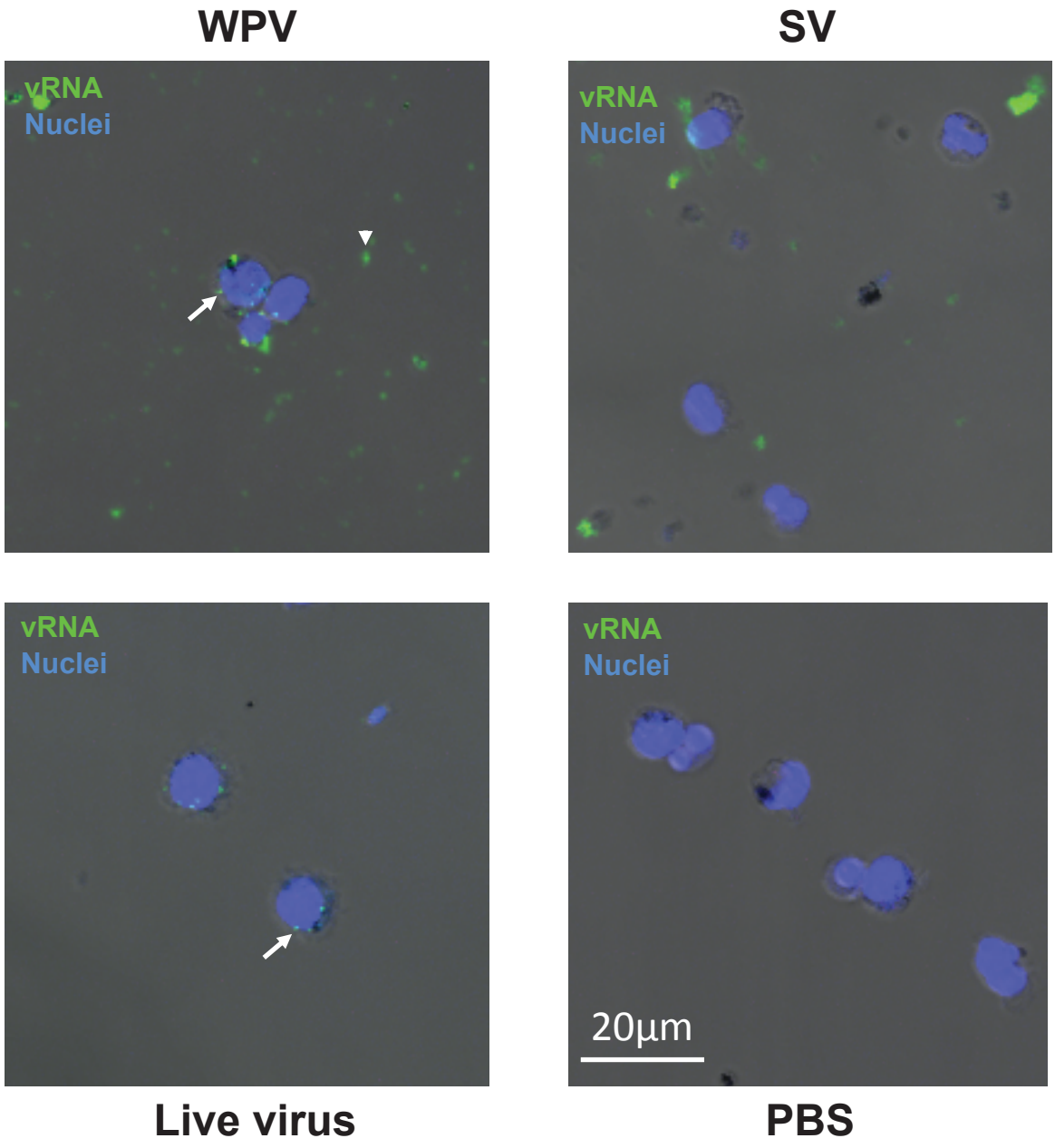

Supplimental figure 2

a)

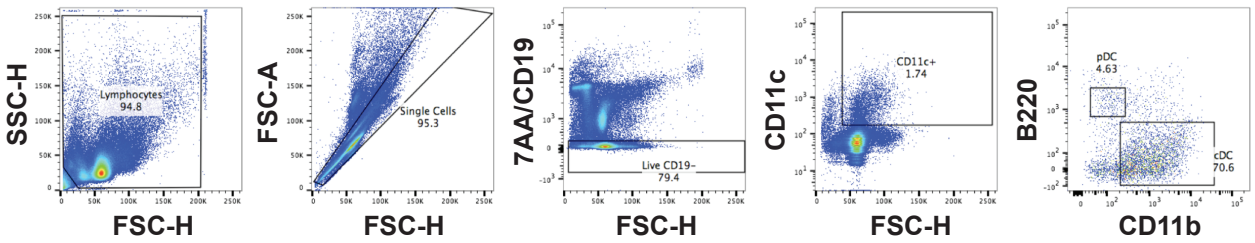

b)

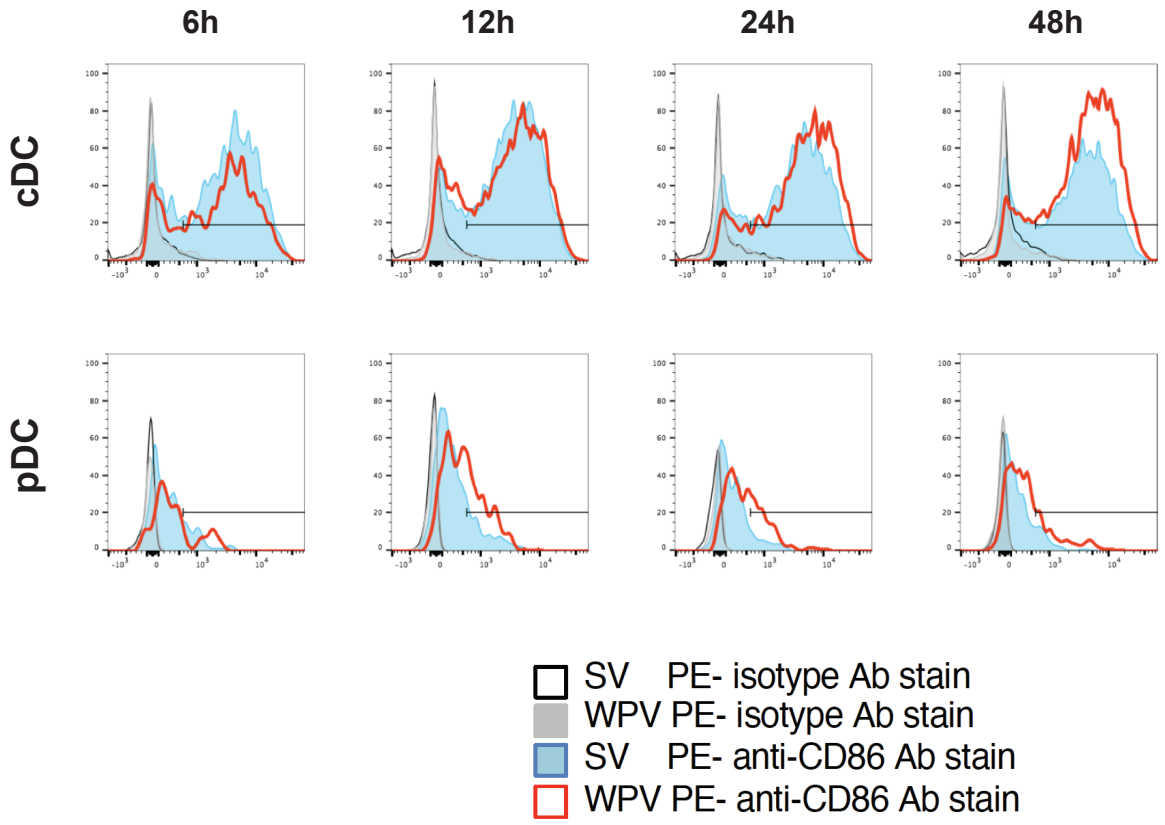

Supplimental figure 3

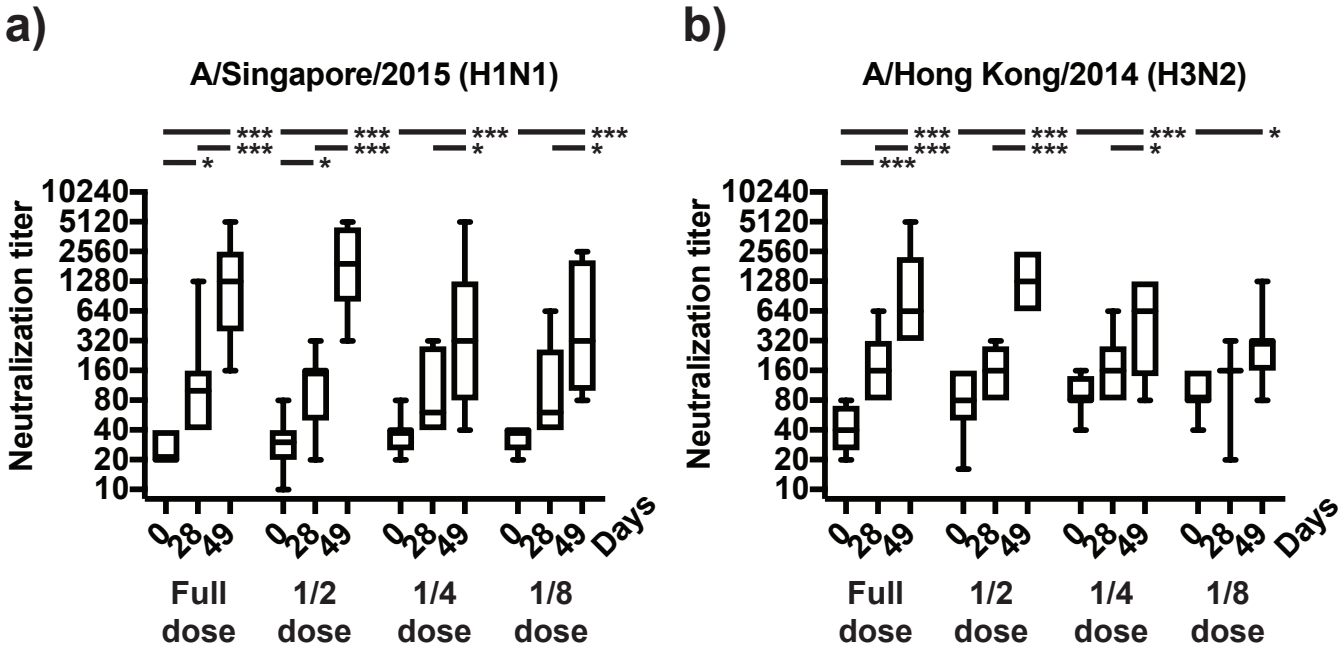

Supplimental figure 4

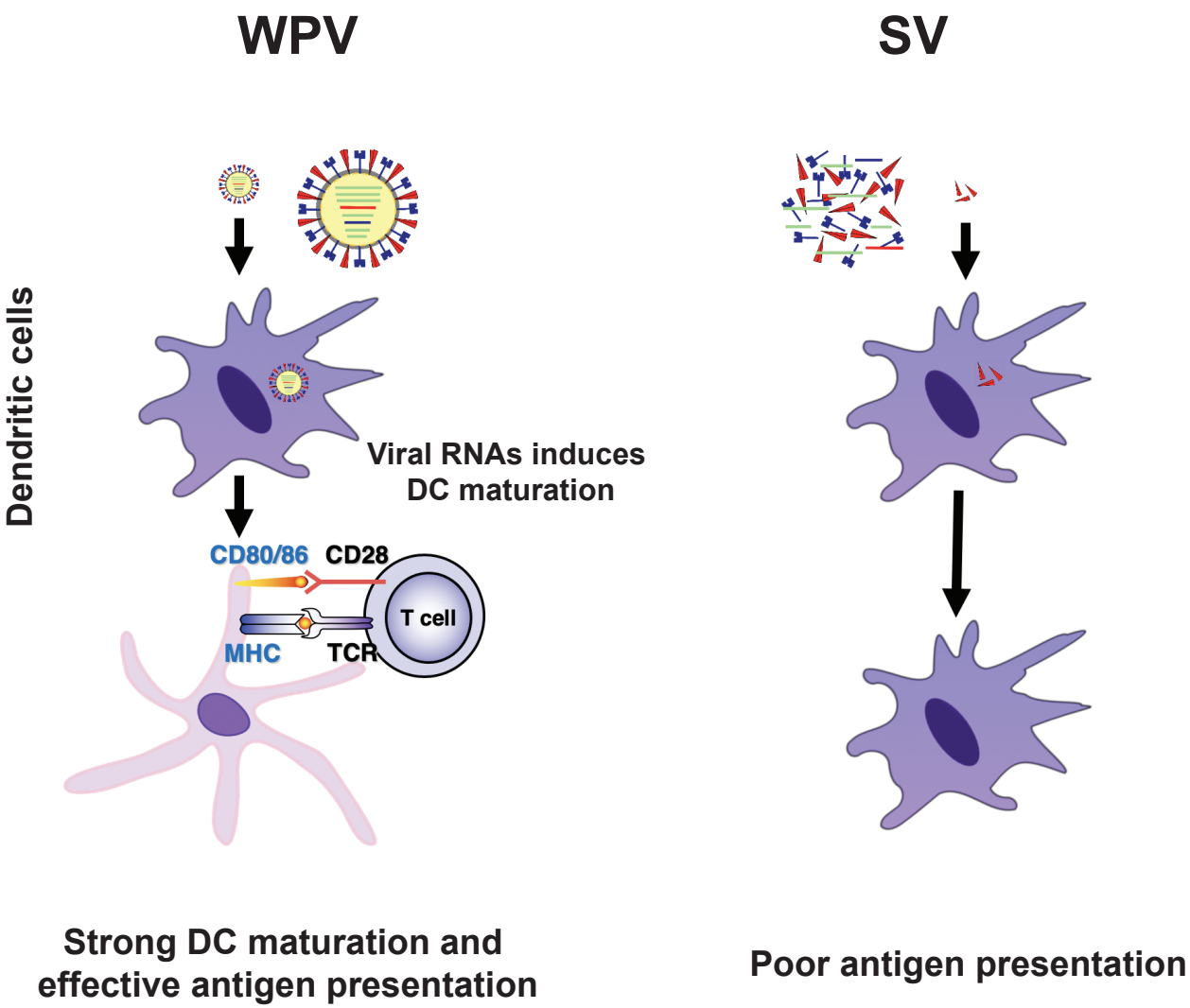

Supplimental figure 5